

Engineering Kidney-Targeted Drug Delivery Systems: Principles, Materials, and Emerging Strategies

Shaogang Wang^{1,*}, Na Zeng^{1,*}, Yuhan Wang², Yuanyuan Yang¹

¹Department of Urology, Tongji Hospital, Tongji Medical College, Huazhong University of Science and Technology, Wuhan, Hubei, 430030, People's Republic of China; ²Department of Laboratory Medicine, Tongji Hospital, Tongji Medical College, Huazhong University of Science and Technology, Wuhan, 430030, People's Republic of China

*These authors contributed equally to this work

Correspondence: Yuhan Wang; Yuanyuan Yang, Email 1195703649@qq.com; tjyangyuanyuan@163.com



Abstract: Kidney-targeted drug delivery is pivotal for treating renal diseases while minimizing systemic toxicity. To navigate the organ's complex physiological barriers, advanced nanomedicines employ integrated strategies. Our comprehensive narrative review provides a structured analysis of these strategies through a dual lens: first, by examining the fundamental mechanisms of renal targeting-including passive filtration, active receptor-mediated uptake, and their synergistic combination; and second, by deconstructing delivery systems into several fundamental pillars, the carrier platforms, the functional moieties that confer targeting, responsiveness and special properties along with therapeutic cargo. We evaluate how polymeric nanoparticles, liposomes, and exosomes, when functionalized with peptides, antibodies, or biomimetic coatings, can achieve enhanced renal specificity. Furthermore, we discuss how microenvironmental triggers such as pH, reactive oxygen species, and enzymes enable precise spatiotemporal drug release at pathological sites. Despite significant progress, critical translational challenges remain, including overcoming hepatic sequestration, ensuring long-term biocompatibility, and addressing patient heterogeneity. Future advances will depend on combining multimodal targeting, real-time feedback, and scalable manufacturing processes. This review synthesizes current knowledge to offer a rational design framework for the next generation of intelligent kidney-targeted therapeutics.

Keywords: kidney-targeted drug delivery, smart nanocarriers, synergistic targeting strategies, stimuli-responsive release

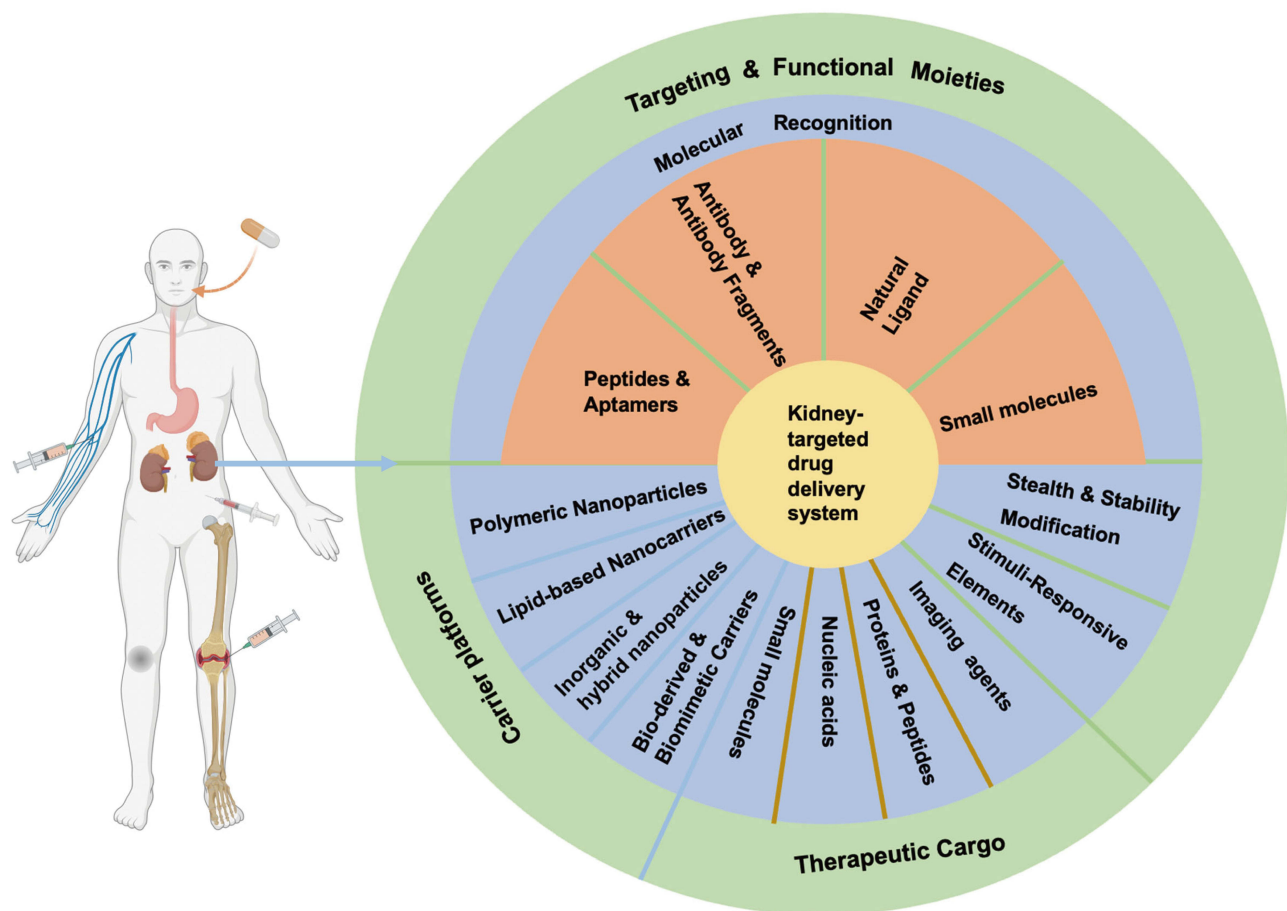
Introduction

Kidney is one of the most vital organs in the human body, it plays important roles in maintaining internal environmental stability, excreting metabolic waste, and regulating various physiological processes.¹ Dysfunction of kidney will lead to many diseases, including renal tumor, kidney stone, acute kidney injury (AKI), chronic kidney disease (CKD), diabetic nephropathy et al.² Kidney disease is a significant global public health issue that has profound impacts on individuals, healthcare systems, and socioeconomic structures. Its high prevalence, disability rates, and mortality make it a pressing health challenge that demands attention and intervention.³

Drug therapy and surgical treatment are the two main treatments for kidney diseases. Drug therapy requires a certain concentration of drugs that eventually reach the kidney to be effective. Unfortunately, kidney is a complex organ with many barriers, which make it hard to deliver to. The vascular endothelial cells within the kidneys form a sieve-like structure. The tight junctions between these cells restrict the passage of large molecules and highly polar substances, while small molecules and lipophilic drugs can pass through more easily.⁴ As drugs pass through the glomerulus, they come into contact with the glomerular basement membrane. The selective filtration function of the basement membrane allows small molecule drugs to pass through, while large molecules or negatively charged drugs may be restricted by its filtration capacity. After drugs enter the renal tubular lumen, they might be reabsorbed across the tubular epithelial cells



Graphical Abstract



into the peritubular capillaries. These cells utilize both active transport and passive diffusion mechanisms.⁵ Importantly, drug entry into renal tissues is not exclusively dependent on glomerular filtration. In addition to the luminal route, therapeutic agents can also access the kidney through the peritubular capillary network, which arises from post-glomerular efferent arterioles. Via this pathway, drugs and nanocarriers in the systemic circulation may directly interact with the basolateral membrane of tubular epithelial cells or renal interstitial compartments, providing an alternative and often dominant route for larger molecules, nanoparticles, and biologics that are not readily filtered by the glomerulus. Moreover, drugs must first travel from the systemic circulation through the renal artery to reach the kidney's blood supply system. The distribution of drugs in the blood may be influenced by their binding affinity to plasma proteins, such as albumin. Drugs with a high protein-binding rate need to be released in their free before they can enter kidney tissues.⁶ The location and physiological anatomy of the kidney pose a certain obstacle to the accumulation of drugs in the kidney.

Thus, the kidney presents a formidable yet valuable target for drug delivery. Successfully navigating its intricate physiological defenses is essential to unlock its full therapeutic potential. Kidney-targeted delivery strategies are designed precisely for this purpose, aiming to guide drugs through these barriers to their site of action, thereby maximizing efficacy and safety.⁷ We divided Kidney-targeted drug delivery system into carrier platforms and Targeting & Functional Moieties. A diverse array of materials, including organic, inorganic, and polymeric nanostructures such as nanoparticles, scaffolds, extracellular vesicles and so on, are served as versatile carriers.⁸ To bestow these carriers with specificity and controllability, various targeting and functional components are employed, including molecular recognition elements, stimuli-responsive materials, and stealth or stability modifiers.⁹ Critically, the design

of an optimal kidney-targeting strategy requires the synergistic integration of these components with a third, equally vital consideration, the therapeutic cargo itself. Only through the rational co-design of the carrier, functional moieties, and the cargo, can a truly effective and smart delivery system be realized.

Therefore, this review aims to provide a comprehensive and updated analysis of smart drug delivery strategies for kidney targeting. Specifically, we seek to synthesize the fundamental mechanisms underlying passive and active renal targeting and critically evaluate the landscape of carrier systems, targeting moieties, and stimuli-responsive designs. What's more, we discuss the synergistic potential of combined strategies and identify persistent challenges and future research directions. By presenting this integrated framework, we intend to guide the rational design of next-generation renal therapeutics and bridge the gap between preclinical innovation and clinical application.

Scope and Methodology of This Review

As a comprehensive narrative review, literature searches in PubMed, Web of Science, and Embase, covering publications from the past decade up to January 2026 were conducted. Key search terms included “kidney targeted drug delivery,” “renal nanoparticle,” “kidney targeting peptide,” “stimuli-responsive renal delivery,” and related variants. Our initial retrieval included studies up to March 2025, from which 117 articles were selected based on their relevance, exemplar status, and contribution to illustrating key concepts or technological advances. In preparing this revised version, we extended the search to January 2026, identifying and incorporating 26 additional pertinent studies. Given the narrative and integrative nature of this review, article selection prioritized conceptual relevance and representativeness rather than adherence to a systematic screening protocol with rigid inclusion/exclusion criteria. The selected literature is analyzed through a conceptual framework that first examines targeting mechanisms, distinguishing between passive and active strategies. Then deconstructs delivery systems into carrier platforms, targeting and functional moieties and stimuli-responsive elements. This structure is designed to offer readers a mechanistic understanding of renal targeting and practical principles for the rational design of kidney-targeted drug delivery system.

Biological Basis of Kidney Targeting

Anatomical Characteristics of Kidney

The kidneys receive more than 20% of the cardiac output, ensuring that the majority of systemically administered drugs are exposed to the renal vasculature. This extensive perfusion facilitates drug transport to nephron units, where filtration, secretion, and reabsorption occur. However, renal exposure alone does not guarantee therapeutic efficacy, as the unique anatomical and biological features of the kidney critically determine whether drugs can access specific renal compartments.

The nephron, the fundamental functional unit of the kidney, consists of the glomerulus and a connected tubular system. The glomerular filtration barrier (GFB) is a highly specialized and dynamic biological interface rather than a simple size-exclusion filter. It is composed of three integrated layers:⁵ fenestrated glomerular endothelial cells, the glomerular basement membrane (GBM), and podocytes with interdigitating foot processes bridged by slit diaphragms. While the endothelial fenestrations (approximately 70–100 nm) facilitate high permeability to water and small solutes, the GBM and slit diaphragm provide charge- and structure-dependent selectivity. Importantly, podocytes do not contain rigid “pores”. Instead, the slit diaphragm represents a complex protein network that functions as a dynamic filtration structure, with an effective size selectivity typically described in functional rather than anatomical terms.¹⁰

Beyond molecular size and charge, increasing evidence suggests that structural features such as molecular architecture and particle geometry can influence interactions with the GFB. Branched or non-spherical nanocarriers may exhibit distinct hydrodynamic behavior and filtration characteristics compared with conventional spherical particles, thereby affecting their ability to traverse or be retained at the glomerular interface.^{11,12} These observations highlight that renal filtration is governed by an integrated interplay of size, charge, and structural organization, rather than a single physical parameter.

As blood flows through the glomerular capillaries, negatively charged macromolecules are partially repelled by the anionic components of the endothelial glycocalyx and GBM, whereas small solutes are freely filtered. Although classical

filtration favors small molecules, it is now well recognized that the GFB can be functionally bypassed or altered under specific physiological and pathological conditions. Mechanisms such as endothelial transcytosis, disease-induced barrier disruption, and enzyme-mediated transport enable larger molecules or nanocarriers to access renal tissues without strict size-dependent filtration.¹³

Following filtration, substances entering the tubular lumen encounter renal tubular epithelial cells, which regulate retention and excretion through passive diffusion and active transport processes. The renal tubule comprises distinct segments, including the proximal tubule, loop of Henle, distal tubule, and collecting duct, each of them exhibits unique transport characteristics. Drug behavior within the tubules is influenced by physicochemical properties such as molecular size, charge, solubility, and pKa, as well as luminal pH and transporter expression.¹⁴ The proximal tubule, in particular, displays high re-absorptive capacity for water-soluble compounds, while distal segments contribute to acid–base balance and selective drug handling.

In addition to the luminal route, renal drug entry is not restricted to glomerular filtration. Therapeutic agents circulating in the bloodstream may also access renal tissues via the peritubular capillary network arising from post-glomerular efferent arterioles. Through this pathway, drugs—especially large molecules, protein-bound agents, and nanocarriers can interact with the basolateral membrane of tubular epithelial cells or enter the renal interstitium, thereby bypass the filtration barrier altogether.¹⁵ Organic anion and cation transporters expressed on tubular cells further mediate active secretion of drugs and metabolites into the tubular lumen.

Collectively, these anatomical and physiological features highlight that renal targeting is governed by multiple, parallel transport routes rather than a single filtration-dependent mechanism (Figure 1). A comprehensive understanding of these pathways is essential for the rational design of kidney-targeted drug delivery systems.

Molecular Mechanisms of Kidney Targeting

Fortunately, the specific molecular expressions enriched in normal or disease kidney, provide several targets with kidney-targeting potential. Several studies^{4,16} have systematically listed common targets which can be categorized into three

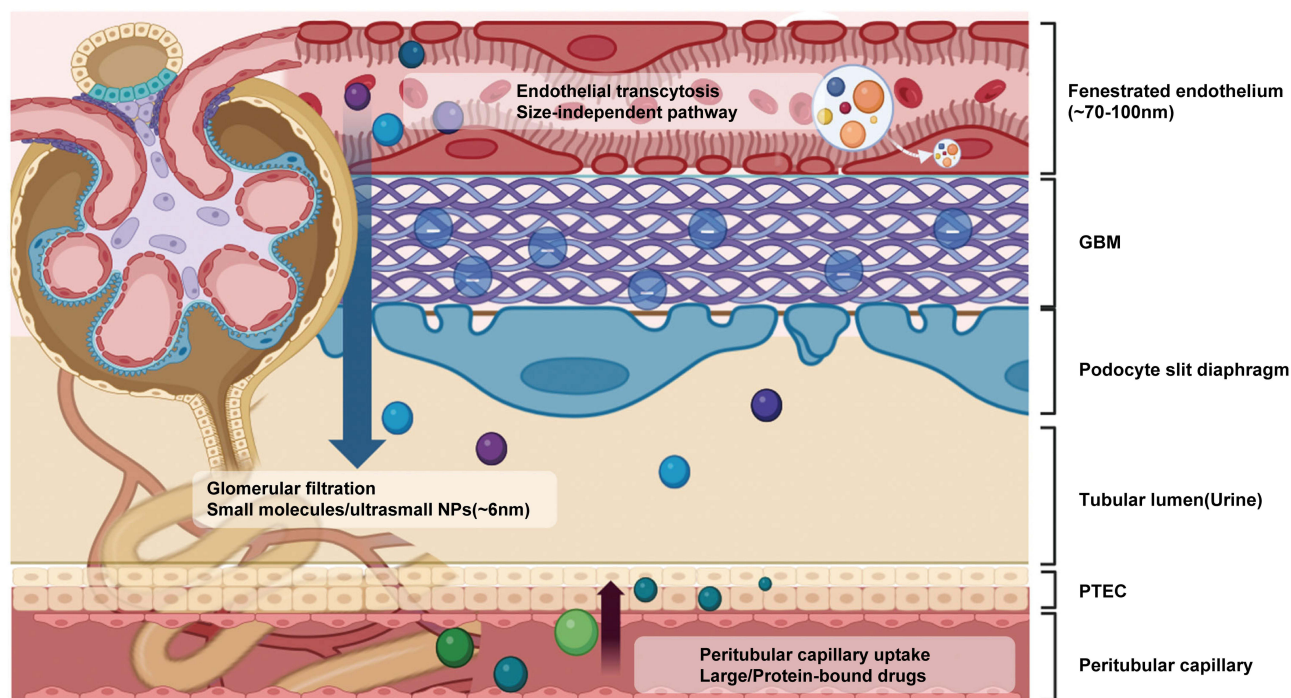


Figure 1 Schematic illustration of renal filtration pathways. Small molecules and ultrasmall nanoparticles (< 6 nm) undergo glomerular filtration through fenestrated endothelium (~70–100 nm) and the glomerular basement membrane (GBM), and are subsequently processed by podocytes and proximal tubular epithelial cells (PTEC). Larger or protein-bound drugs are primarily cleared via endothelial transcytosis, a size-independent pathway, entering peritubular capillaries and undergoing tubular luminal and peritubular capillary uptake. The arrows correspond to the primary directional pathways described above.

main groups: First, targeting proteins highly expressed in podocytes, including FcRn,^{17,18} VCAM-1,^{19–21} and $\alpha\text{v}\beta 3$,^{12,22} second, targeting E-selectin and P-selectin on endothelial cells (ECs),^{23,24} third, targeting megalin and cubilin on proximal tubular epithelial cells (PTECs).^{25,26} By modifying delivery systems to target these molecules, it is possible to enhance affinity with renal cells and increase drug uptake.

Physiological Changes in Kidney Disease States

In pathological conditions, the normal structure and function of the kidneys are impaired, leading to three typical changes: alterations in the renal microvascular network resulting in decreased renal blood flow, damage to the filtration barrier causing excessive filtration of macromolecules, and changes in renal enzyme activity leading to dysregulation of small molecule transport. These changes present both challenges and opportunities for targeting kidney disease. For example, in acute kidney injury (AKI), renal blood flow (RBF) can decrease by 50–60%, and microvascular permeability increases.²⁷ On one hand, the reduction in blood flow decreases the bioavailability of drugs in the kidneys, and the prolonged residence time increases the potential risk of toxicity. On the other hand, the increased permeability of the glomerular filtration barrier (GFB) allows larger nanoparticles to pass through, promoting their accumulation in the kidneys. Additionally, kidney diseases are often associated with changes in the expression and activity of key proteins. For instance, in diabetic nephropathy (DN), the high expression of the renal tubular transporter NHE3 leads to increased sodium ion retention,²⁸ while in renal failure, the accumulation of metabolic waste products and local inflammation suppress the expression of organic anion transporters (OAT1–4),²⁹ further exacerbating toxin accumulation. However, the high reactive oxygen species (ROS) environment provides an opportunity for the design of ROS-responsive kidney-targeting particles,³⁰ and targeting inflammatory cells allows for more precise delivery of drugs to injured kidney cells.^{31,32} In renal cell carcinoma (RCC), the high expression of CAIX and CD70 has also emerged as potential targeting sites^{33–35} (Figure 2).

Mechanisms and Strategies of Kidney-Targeted Drug Delivery Systems

Kidney Passive Targeting

As mentioned above, the physicochemical properties of drug carriers, particularly size, shape and surface charge, critically influence their renal distribution routes, including glomerular filtration, endothelial transcytosis, and tubular uptake. Factors such as solubility, affinity, and pH further affect drug secretion and reabsorption along the nephron. Importantly, renal passive targeting should not be viewed as a rigid size-threshold-dependent process, but rather as a dynamic and route-dependent phenomenon shaped by both particle properties and renal physiological status.

Regarding molecular size, for kidney-specific targeting, particles must be sufficiently large to avoid rapid clearance from the body when distributed in the renal tubules (> 2 nm), but small enough to reduce, rather than completely prevent nonspecific uptake by the liver, spleen, or lungs (< 100 – 1000 nm).³⁶ Generally, nanoparticles with a diameter less than 6 nm and proteins with a hydrodynamic diameter (HD) less than 6 nm can successfully pass through the glomerular filtration barrier^{4,15,37} and are cleared via renal excretion. Nanoparticles around 10 nm temporarily enter the mesangium, but due to the lack of phagocytosis, they do not remain there, while particles larger than 20 nm are less likely to accumulate in the kidneys.¹⁶

Notably, renal targeting behavior of ultrasmall nanoparticles is highly sensitive to disease associated alterations in renal clearance pathways. For example, PEGylated glycyrrhizic acid-based nanoparticles (~ 4.5 nm) exhibit rapid renal elimination in healthy mice due to their size being below the filtration threshold.³⁸ However, in acute kidney injury (AKI) models, impaired tubular clearance and obstructive damage result in enhanced renal retention of the same nanoparticles, as visualized by *in vivo* PET imaging. This phenomenon exemplifies a size-gated yet disease triggered passive targeting mechanism, in which particle size determines filterability, while pathological conditions dictate final renal distribution.

Although classical filtration favors small nanoparticles, renal accumulation of larger particles has also been reported under specific experimental or pathological contexts. Williams et al observed that nanoparticles with a diameter of about 400 nm showed 7 times higher targeting efficiency in the kidney compared to the heart, lungs, spleen, and liver.³⁹ Similarly, micron-sized microcapsules (~ 3 μm) have been shown to localize within the kidney under renal-targeted

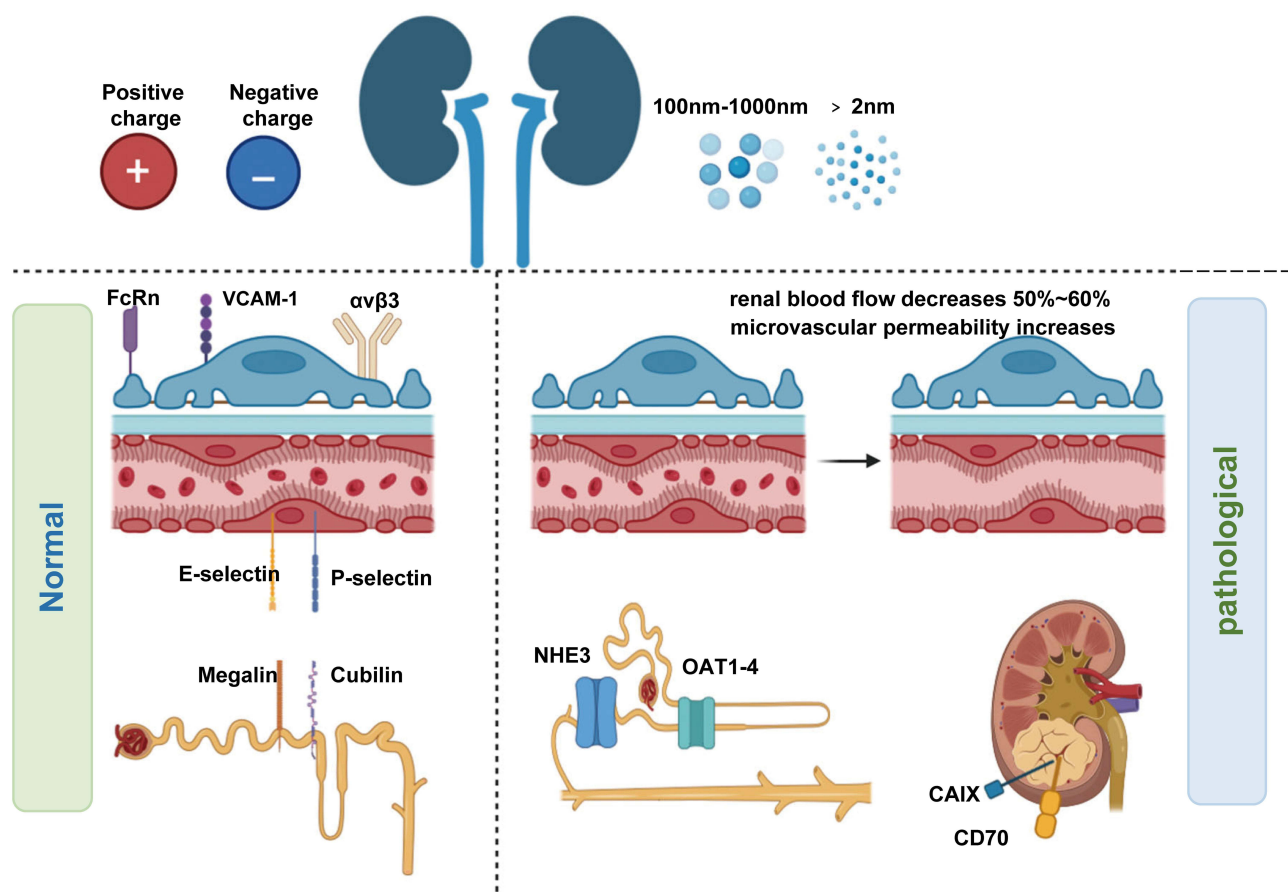


Figure 2 Impact of renal pathophysiological changes on drug delivery. In pathological conditions, three typical changes might happen: alterations in the renal microvascular network resulting in decreased renal blood flow, damage to the filtration barrier causing excessive filtration of macromolecules, and changes in renal enzyme activity. In addition, kidney diseases are often associated with changes in the expression and activity of key proteins which might be targets for kidney drug delivery.

administration conditions.⁴⁰ Importantly, such renal localization was achieved under renal artery or kidney-targeted administration rather than systemic intravenous injection, and therefore should not be generalized to conventional passive targeting strategies. Such observations are generally attributed to non-filtration-based mechanisms, including mechanical trapping within glomerular capillaries, altered hemodynamics, or direct access from peritubular capillaries, rather than conventional size-dependent filtration.

For ultrasmall nanoparticles (<5.5 nm), surface charge becomes a dominant determinant of renal fate.¹⁶ Negatively charged quantum dots (~3.7 nm) preferentially accumulate in mesangial cells, whereas similarly sized cationic quantum dots (~5.67 nm) are rapidly excreted into urine. For larger nanoparticles, renal accumulation is often mediated by active uptake in renal tubules.¹⁵ Due to the negatively charged microvilli densely covering the luminal surface of proximal tubule epithelial cells (PTECs), positively charged nanoparticles exhibit enhanced retention and uptake in proximal tubules compared with neutral or negatively charged counterparts.^{41–44}

Beyond size and charge, particle geometry has recently emerged as an additional modulator of renal passive targeting behavior. Nanostructures with distinct shapes, such as dendrimers⁴⁵ or DNA origami architectures,¹⁵ interact differently with glomerular flow dynamics and filtration barriers. Dendritic macromolecules, owing to their highly branched and monodisperse architecture, offer tunable size and surface functionality but may exhibit charge-related toxicity with increasing generation. Meanwhile, shape-defined DNA nanostructures with rectangular, triangular, or tubular geometries have demonstrated unexpected renal clearance and therapeutic efficacy in AKI models, despite dimensions exceeding classical filtration limits. These findings suggest that particle shape may influence renal transport by modulating

hydrodynamic behavior, deformation, and barrier interactions, although the underlying mechanisms remain incompletely understood.

Kidney Active Targeting

However, passive targeting often fails to meet the demands for renal targeting in many cases, as non-specific drug distribution increases the risk of systemic side effects. Since these large nanoparticles also exhibit high non-specific distribution, loading targeting ligands into the delivery system is an optimal strategy to further improve renal targeting. Whether directly conjugated with therapeutic agents⁴⁶ or integrated into nanoparticle carriers,^{47–50} these strategies have demonstrated enhanced renal accumulation. In addition to targeting peptides, antibodies and natural ligands can also be utilized for active kidney targeting, the category and function of these modification are thoroughly discussed in Targeting and Functional Moieties below. Moreover, due to the abundant expression of specific markers in the kidney diseases, various modification targeting specific markers have shown excellent renal targeting capabilities. For example, the expression of CD44 on renal cells with inflammation is abnormally upregulated.⁵¹ Zhi-Wei Huang et al⁵² developed hyaluronic acid-coated ϵ -polylysine–bilirubin conjugated nanoparticles that can target CD44 on damaged renal cells and selectively accumulate in the damaged kidneys.

Beyond classical ligand-receptor-mediated endocytosis in tubular epithelial cells, emerging evidence indicates that renal active targeting can also be achieved by promoting glomerular endothelial transcytosis. Recent studies have demonstrated that short amino acid repeat peptides, single amino acid modifications, or prodrug-like surface displays can facilitate carrier transport across the glomerular endothelium via active transcellular pathways rather than passive size dependent filtration. For example, enzyme-activatable dendrimer-drug conjugates responsive to γ -glutamyl transpeptidase (GGT), a brush-border enzyme enriched in glomeruli, enable site-specific drug activation and efficient glomerular delivery through receptor-mediated transcytosis, thereby overcoming physiological filtration barriers.⁴⁵ Similarly, serine-modified nanocarriers have been shown to enhance glomerular accumulation while reducing hepatic uptake, highlighting the critical role of minimalistic amino acid motifs in regulating endothelial transport behavior.⁵³

In parallel, exosome and small extracellular vesicle (sEV) based delivery systems have emerged as a unique class of renal-targeting nanotherapeutics that combine both passive and active targeting features. Engineered exosomes derived from mesenchymal stem cells or immune cells exhibit intrinsic renal tropism and can be further functionalized to enhance kidney specificity. These vesicles are capable of traversing renal endothelial barriers, evading rapid clearance, and delivering bioactive cargos to glomerular or tubular cells. Recent studies have demonstrated that surface-engineered EVs achieve superior renal accumulation and therapeutic efficacy in models of acute kidney injury and chronic kidney disease, underscoring their potential as next-generation kidney-targeted delivery platforms.

Notably, despite the improved specificity conferred by active targeting strategies, several intrinsic limitations remain.⁵⁴ First, ligand or peptide modification may increase immunogenicity and accelerate systemic clearance. Wilson W. K. Cheng et al⁵⁵ found that antibody-modified liposomes exhibited 4-5-fold higher blood clearance rates compared to non-targeted counterparts. Second, many active targeting pathways rely on endocytosis, which may lead to lysosomal degradation of encapsulated biologics, such as proteins or nucleic acids, thereby compromising therapeutic efficacy.⁵⁶ These challenges highlight the necessity of integrating transcytosis-based transport, enzyme-responsive activation, and vesicle-mediated delivery to optimize renal targeting outcomes. Importantly, active targeting rarely overrides the fundamental constraints imposed by renal passive targeting, and in most cases only marginally enhances renal accumulation within the physicochemical boundaries established by carrier size, charge, and circulation behavior. Therefore, passive and active targeting should not be viewed as independent strategies, but as interdependent design layers that must be co-optimized.

Interplay Between Passive and Active Targeting Strategies

Rather than functioning as two independent modules, passive and active targeting strategies are mechanistically interdependent in kidney-targeted drug delivery systems. Passive targeting, governed by particle size, shape, surface charge, and circulation behavior, determines the initial renal exposure of drug carriers, whereas active targeting primarily refines cellular or sub-organ localization within the constraints imposed by passive biodistribution.

In this context, drug carriers with inherent renal accumulation properties can provide a favorable biodistribution background, upon which ligand-mediated targeting further enhances specificity. For example, elastin-like polypeptide (ELP), a carrier known for its preferential renal uptake, is frequently combined with kidney-targeting peptides (KTPs). PEG–PLGA vesicles exhibit prolonged circulation and reduced nonspecific uptake due to steric stabilization. However, PEGylation may also reduce cellular internalization efficiency.⁵⁷ Surface modification compensates for this limitation by enhancing renal cellular uptake, illustrating that active targeting serves to locally amplify the passive renal exposure conferred by PEGylation rather than replacing it.^{26,47}

Notably, as we described above, EVs and exosomes represent an emerging renal delivery paradigm in which passive and active targeting mechanisms are intrinsically integrated. Native and engineered exosomes possess favorable biodistribution characteristics, including nanoscale size and prolonged circulation, while their membrane proteins and engineered surface ligands enable cell-specific uptake and endothelial interactions. Exosome-based delivery systems have demonstrated robust renal accumulation and therapeutic efficacy in multiple kidney disease models, including ischemia–reperfusion injury, chronic kidney disease, renal fibrosis, and anemia.^{58–63}

Collectively, these findings underscore that passive and active targeting strategies are not independent or interchangeable, but rather represent a continuous targeting spectrum shaped by renal physiology and transport mechanisms (Figure 3).

Engineering Building Blocks for Kidney-Targeted Delivery Systems

The rational design of effective kidney-targeted nanomedicines requires a understanding of its core components. This section deconstructs the delivery system into several fundamental pillars, the carrier platforms, the functional moieties that confer targeting, responsiveness, and special properties along with the therapeutic cargo. The ultimate therapeutic efficacy arises from the intelligent integration of these parts.

Carrier Platforms

The materials of carriers decide the fundamental pharmacokinetics, biocompatibility, drug capacity and interaction with biological barriers.

Polymeric Nanoparticles (NPs)

Polymeric Nanoparticles, typically ranging from 10 to 1000 nm, consisting of a solid core surrounded by suitable chemicals that can influence their size and polarity.⁶⁴ The polymeric materials employed are extensive, primarily encompassing PLGA, cationic natural polymers, synthetic polycations and various functional copolymers or hybrid systems. To provide an overview of this vast landscape, key representative studies are compiled in Table 1.

Poly(Lactic-Co-Glycolic Acid) (PLGA)

Polymeric NPs, particularly those based on biodegradable poly(lactic-co-glycolic acid) (PLGA), are among the most extensively studied carriers due to their excellent biocompatibility, controllable drug release profiles, and ease of surface functionalization. For instance, PLGA NPs loaded with oltipraz demonstrated specific and prolonged retention in ischemic-reperfusion (IR) injured kidneys for up to 10 days,⁷¹ while cabozantinib-loaded PLGA NPs (CZ-PLGA-NPs) showed promise as a targeted adjuvant for renal cell carcinoma (RCC) therapy.⁶⁶ Surface modification with polyethylene glycol (PEG) is a pivotal strategy to enhance hydrophilicity, prolong circulation, and reduce hepatic and splenic clearance.³⁶ This is exemplified by PEG-PLGA nanoparticles (FNPs, 400–500 nm) that showed 26-fold greater kidney-to-heart fluorescence ratio in injured kidneys, primarily relying on passive, pathology-enhanced permeability.⁶⁷ Similarly, PEGylated PLGA nanoparticles effectively delivered formoterol to renal tubules in the cortex,⁶⁹ and PEG-PLGA-DiR NPs showed enhanced and sustained accumulation in unilateral ureteral obstruction (UUO) kidneys compared to free dye.⁶⁸ An optimal particle size for renal accumulation within the PLGA-PEG system was suggested to be around 90 nm.⁷² Hybrid approaches, such as PLGA nanoparticles coated with chitosan and then modified with a kidney-targeting peptide (KTP) and hyaluronic acid, have also demonstrated strong kidney-specific targeting and accumulation within 24 hours.⁷³ Furthermore, modifications with various targeting peptides, including KTPs, can substantially enhance

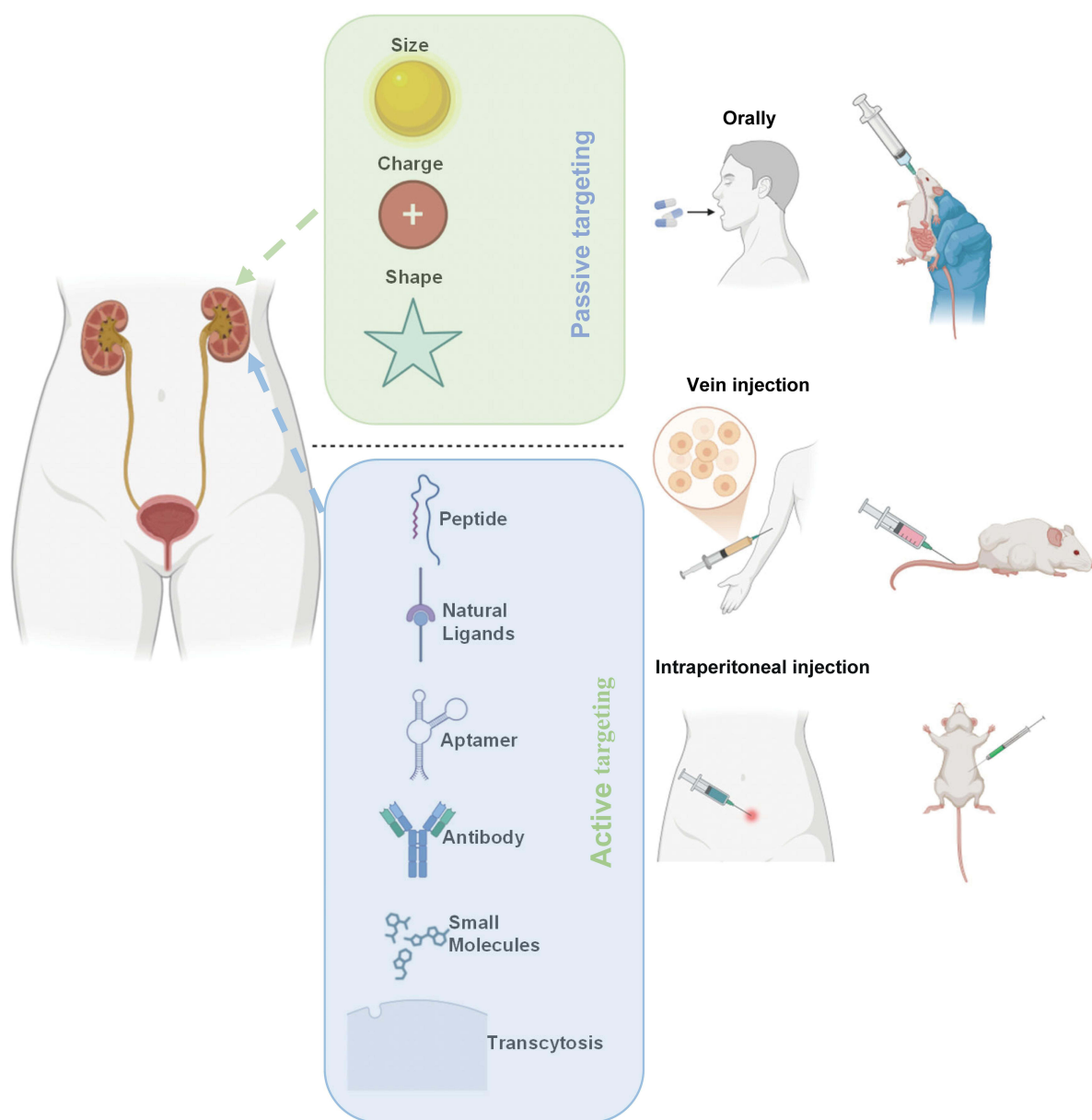


Figure 3 Mechanisms and strategies of kidney-targeted drug delivery systems. The working modes of renal-targeted delivery systems are primarily categorized into active targeting and passive targeting. Passive targeting mainly depends on the size, charge and shape of drugs or carriers. Appropriate dimensions, positive charges and special shapes can enhance renal passive targeting efficiency. Active targeting refers to transcytosis of epithelial cells or the design of ligands that specifically target kidney biomarkers. The optimal renal targeting effect can only be achieved through the combination of active and passive targeting strategies.

renal targeting efficiency,^{47,65} and these specific modification strategies will be discussed in detail in the following section. Additionally, innovative combination strategies, such as complexing PLGA-RSG nanoparticles with SonoVue microbubbles (MBs) to form PLNPs-RSG-MBs, have been developed. Upon ultrasound exposure, this combination strategy was shown to significantly improve renal drug deposition compared to nanoparticles alone, highlighting the potential of physical targeting modalities.⁷⁰

Cationic Polymers

Cationic polymers exploit electrostatic interactions with the negatively charged glomerular structures to enhance renal retention. Chitosan, a natural polysaccharide derived from chitin, is a prominent example widely used in renal targeting due to its biodegradability, biocompatibility, and inherent positive charge. This cationic nature facilitates its accumulation

Table I Polymeric Nanoparticles

PMID	Year	Author	Carrier	Methods	Biodistribution	Model	Detection	Administration
38956234 [ref: ³⁶]	2024	Takamitsu Saigusa	Poly lactic-co-glycolic acid (PLGA) Nanoparticles (NPs)	MNPS were composed of PLGA (polylactic acid-glycolic acid) and PEG (polyethylene glycol) with an average particle size of 350 nm.	Immunofluorescence results showed that PEG-modified MNPS were able to accumulate in the renal cortical regions, especially in cystic and non-cystic renal tubular epithelial cells	Mouse	IF	Intravenously injection (1mg/kg, tail vein), bi-weekly for 6weeks
35429575 [ref: ⁶⁵]	2022	Yunching Chen	Poly lactic-co-glycolic acid (PLGA) Nanoparticles (NPs)	Engineered lipid-coated poly(lactic-co-glycolic acid) nanoparticles (NPs) with fibrotic kidney-homing peptides on the surface	The peptide-modified NPs reached the UUO-induced fibrotic kidneys as much as 2.6-fold higher than the non-targeting NPs.	Mouse	Fluoroskan Ascent FL	Intravenously injection (20 mg/kg, tail vein)
36293494 [ref: ⁶⁶]	2022	Seong Il Seo	Poly lactic-co-glycolic acid (PLGA) Nanoparticles (NPs)	Cabozantinib was encapsulated into PLGA nanoparticles by conventional single emulsion technique	As a novel nanoplatform, CZ-PLGA-NPs have multi-dimensional anti-metastatic effects and are able to reduce non-targeted toxicity, which is a promising adjuvant treatment strategy for high-risk post-nephrectomy RCC patients.	Mouse	IVIS Spectrum	Intravenously injection (10mg/kg, tail vein)
35779607 [ref: ⁶⁷]	2022	Rick G. Schnellmann	PLGA-PEG nanoparticles	Nanoparticles (FNPS) with a diameter of 400–500 nm were prepared using PLGA-PEG as the carrier material. Nanoparticle surface PEG modification reduced liver and spleen clearance and improved renal enrichment.	The fluorescence signal of FNP was significantly stronger in the kidney than in other organs such as the heart and liver, especially in damaged kidney tissue. The fluorescence signal in the kidney was 26 times greater than that in the heart, indicating that the enrichment of nanoparticles in the kidney was mainly dependent on the pathological permeability enhancement at the lesion site	Mouse	IVIS Spectrum	Intravenously injection (0.04mg/kg, tail vein)

34529980 [ref: ⁶⁸]	2021	Hongmei Zang	PLGA-PEG nanoparticles	Gypenoside XLIX (Gyp XLIX) was dissolved in methanol using poly lactic-co-glycolic acid (PLGA), lecithin, and methoxy polyethylene glycol-distearylphospholipid ethanolamine (mPEG-DSPE) as raw materials, and then added to the organic phase of PLGA as described above.	Fluorescence imaging results showed that PLGA-DiR NPs accumulated more in the UJO kidneys and had a longer duration of fluorescence compared to the free DiR solution. At the third day after injection of PLGA-DiR NPs, DiR fluorescence intensity was stronger in the UJO kidneys of the PLGA-DiR NPs group compared with the DiR solution group, and fluorescence was still detectable in the UJO kidneys at the seventh day.	Mouse	IVIS Spectrum	Intravenously injection (5mg/kg, tail vein)
34169439 [ref: ⁶⁹]	2021	Heidi M. Mansour	PLGA-PEG nanoparticles	Poly(ethylene glycol) methyl ether-block-poly(lactide-co-glycolide) nanoparticles containing encapsulated formoterol were synthesized by a modified single-emulsion solvent evaporation technique resulting in nanoparticles with a median hydrodynamic diameter of 442 nm.	The PLGA-PEG nanoparticles were successfully localized in the renal tubules of the renal cortex in mice. By staining kidney sections with an anti-polyethylene glycol (PEG) antibody, investigators observed distribution of nanoparticles in renal tubules but not in glomeruli or endothelial cells.	Mouse	IF	Intravenously injection (40µg/kg, tail vein)
32464235 [ref: ⁴⁷]	2020	Ninghua Tan	Poly lactic-co-glycolic acid (PLGA) Nanoparticles (NPs)	Applied PLGA microspheres as carriers and modified them with fluorescein isothiocyanate (FITC) labeled KTP via PEG from outside (KTP-NPs)	Quantitative analysis of fluorescence intensity showed that KTP increased accumulation level of NPs 30-fold relative to that of NPs alone, and of note, heart distribution was also enhanced but inferior to kidney	Rat	Ex vivo organ imaging	Intravenously injection (4 mg/kg, tail vein)

(Continued)

Table 1 (Continued).

PMID	Year	Author	Carrier	Methods	Biodistribution	Model	Detection	Administration
33061383 [ref: ⁷⁰]	2020	Bin yang	Poly lactide-co-glycolide (PLGA) nanoparticles	Poly lactide-co-glycolide (PLGA) nanoparticles were used to load PPAR γ agonist (rosiglitazone, RSG) and prepare PLGA-RSG nanoparticles (PLNPs-RSG); then, a novel complex between PLNPs-RSG and SonoVue microbubbles (MBs) (PLNPs- RSG-MBs) was prepared.	The biodistribution of PLNPs-RSG-Cy5.5 or PLNPs-RSG-MBs-Cy5.5 was evaluated in a rat model of unilateral ureteral obstruction (UUO) using a near-infrared (NIR) imaging system. It was found that the fluorescence intensity of the PLNPs-RSG-MBs complex after ultrasound exposure was stronger in the kidney compared to the group without ultrasound exposure, indicating that ultrasound exposure can improve the renal accumulation of the pair complex.	Mouse	IVIS Spectrum	Intravenously injection (30mg, tail vein)
31349200 [ref: ⁷¹]	2019	Xiaozhi Zhao	Poly lactide-co-glycolide (PLGA) nanoparticles	Designed PLGA NPs loaded with Oltipraz (PLGA-Oltipraz NPs)	The relative fluorescence intensity in the IR kidney was 45%, 31%, 32%, 32%, 41%, and 52% at 3, 12, 24, 48, 72 hours, and 7 days after injection, respectively. These results indicate that PLGA NPs can specifically target the IR kidney and can remain in the IR kidney for at least 10 days to achieve sustained drug release.	Mouse	IVIS spectrum	Intravenously injection (5 μ g, tail vein)
29950614 [ref: ⁷²]	2018	Ling Zhang	PLGA-PEG nanoparticles	Developed a novel PEG-PLGA nanoparticle delivery system capable of delivering dexamethasone acetate (A-DEX)	The results showed that the fluorescence intensity of 70 nm, 90 nm, and 110 nm DiD-nps increased in all imaging organs compared to the free DiD solution. In particular, in the kidney, there was a significant difference in signal intensity between different sizes of DiD-NPs, with 90 nm DiD-NPs being more localized in the kidney	Rat	IVIS spectrum	Intravenously injection (50 μ g/kg, tail vein)

38688026 [ref: ⁷³]	2024	Xiao-cong Zuo	PLGA & Chitosan	Use PLGA as the core of the nanoparticles, the nanoparticles were first coated with cationic chitosan (CS), then Arg-2 siRNA, and finally coated with anionic hyaluronic acid (HA). The renal targeting and accumulation were enhanced by modifying the outermost layer of HA with a kidney-targeting peptide (KTP)	The results showed that the fluorescence signal of KTP-modified nanoparticles was the strongest in the kidney, and the signal was only detectable in the kidney within 24 hours, indicating its high kidney targeting. Organ fluorescence imaging and immunofluorescence analysis further confirmed the accumulation of nanoparticles in the kidney, especially the specific uptake of proximal convoluted tubules.	Mouse	IVIS Spectrum & IF	Intravenously injection 0.5mg/kg, tail vein)
39240782 [ref: ⁷⁴]	2024	Yao Fu	Chitosan	Designed a chitosan oligosaccharide derivative by conjugating COS with stearic acid via an amide linkage and then prepared CLT-loaded COS-SA micelles (COS-SA/CLT), then different proportions of human serum albumin (HSA) were adsorbed onto the surface of COS-SA/CLT to yield COS-SA/CLT@HSA.	Mice treated with COS-SA/DiD or COS-SA/DiD@HSA showed significantly higher fluorescence intensity in the kidneys than that of free DiD, demonstrating that COS-SA had good renal targeting ability and HSA corona did not affect its renal targeting potential. What's more, the formation of the HSA corona was conducive to a greater distribution of the micelles in the renal tubules.	Mouse	IVIS Spectrum	Intravenously injection (0.4mg/kg)
35714868 [ref: ⁷⁵]	2022	Chaitali Prajapati	Chitosan	N-acetylated chitosan nanoparticles containing thymoquinone	The maximum amount of TQ-NP was found in the kidneys for up to 12 h	Rat	Fluorescence microscopy	Intravenous injection (5mg/kg)

(Continued)

Table 1 (Continued).

PMID	Year	Author	Carrier	Methods	Biodistribution	Model	Detection	Administration
35552115 [ref: ⁷⁶]	2022	David Oupický	Chitosan	A new cationic polymer, C-CS, was synthesized for siRNA delivery by combining α -cyclohexyl-p-trocholic acid (CPTA) with chitosan (CS). C-CS has the property of targeting and antagonizing CXCR4 overexpressing cells.	In the injured kidney, the C-CS/siRNA nanoparticles accumulated about 2.5 times as much as in the normal kidney, while the accumulation of siRNA was about 1.5 times as much as in the normal kidney, indicating that the C-CS/siRNA nanoparticles were targeted to the injured kidney. In addition to the kidney, C-CS/siRNA nanoparticles were also distributed in the liver and spleen, but mainly accumulated in the damaged kidney	Mouse	IVIS Spectrum	Intravenously injection (16 μ g, tail vein)
33483059 [ref: ⁷⁷]	2020	Yu-Fen Zhao	Chitosan	Design stepwise-targeting chitosan oligosaccharide, triphenyl phosphine-low molecular weight chitosan-curcumin (TPP-LMWC-CUR, TLC)	TLC showed significant renal targeting ability in vivo. Using fluorescence imaging, the researchers examined the distribution of TLC in mice with AKI. The accumulation of TLC in the kidney peaked at 6 h after administration and showed a stronger fluorescence signal than free CUR, curcumin, indicating a high concentration of TLC in the kidney.	Rat	IHC	Intravenously injection (4mg/kg, tail vein)
24862442 [ref: ⁷⁸]	2014	Qineng Ping	Chitosan	Form coordination-driven assembly from catechol-derived low molecular weight chitosan (HCA-Chi), metal ions and active drug molecules.	Relative uptake rate of kidney from AUC ratio of nanocomplex group to free DOX group was calculated as 25.6, confirming that HCA-Chi- Cu-DOX ternary nanocomplex did possess significant capacity in kidney targeting.	Mouse	IVIS Spectrum	Intravenously injection (5mg/kg, tail vein)
38000609 [ref: ⁷⁹]	2023	Wei Xiong	PEGylated chitosan (PCS)	A variety of PEGylated chitosan (PCS) were synthesized, and the best PCS copolymer was screened for the preparation of SalB-PCS-NPs	The accumulation of FITC-PCS-nps in the kidney was 4.6-fold higher than that of free FITC and 2.1-fold higher than that of FITC-CS-nps, confirming that the developed PCS-NPs successfully enhanced renal targeting distribution	Mouse	IVIS Spectrum	Orally (30mg/kg)

33276016 [ref: ⁴⁰]	2021	Olga A Sindeeva	Poly-L-arginine and dextran sulfate	Prepare Cy7-Conjugated BSA and RITC-Conjugated BSA and use calcium carbonate microspheres as templates to make fluorescent capsules.	Efficacy of fluorescent dye localization in the target kidney after intra-arterial administration is 9 times higher than in the opposite kidney and after intravenous injection.	Mouse	IVIS Spectrum	Intra-arterial injection (20*10 ⁶ capsules)
36145694 [ref: ⁵³]	2022	Akira Yamamoto	L-serine (Ser)- modified poly-L- lysine (PLL)	Investigators have synthesized L-serine (Ser) -modified poly-L-lysine (PLL) to develop a biodegradable renal-targeting drug carrier for effective radionuclide therapy of RCC.	In mice, approximately 91% of the total dose accumulated in the kidney within 3 h after intravenous administration of ¹¹¹ In-labeled Ser-PLL. SPECT/CT showed that ¹¹¹ In-labeled Ser-PLL accumulated in the renal cortex after intravenous injection. Intrarenal distribution studies showed that fluorescein isothiocyanate (FITC) -labeled Ser-PLL mainly accumulated in the proximal convoluted tubules.	Mouse	SPECT/CT	Intravenously injection (1mg/kg, tail vein)
38970881 [ref: ⁸⁰]	2024	Anupama Mittal	Polymeric CPep Nano complexes (NPX)	NPX is formed by the electrostatic interaction between positively charged polymer nanospheres (BNP) and negatively charged C-peptide. NPX has a particle size of about 167 nm and a slight positive charge (+10.3 mV), which is suitable for cellular uptake through the renal tubular epithelium.	NPX accumulation in the kidney was significantly increased compared with free C-peptide. The improved stability and prolonged half-life of NPX led to a significant increase in its renal concentration, NPX could efficiently accumulate in the kidney and pancreas of diabetic rats, showing good targeting ability.	Rat	Pharmacokinetics and IHC	Intravenously injection (1 μg/kg, tail vein)

(Continued)

Table 1 (Continued).

PMID	Year	Author	Carrier	Methods	Biodistribution	Model	Detection	Administration
38940537 [ref. ⁸¹]	2024	Yongping Zhang	Cationic polymeric nanoparticles (PPS-CPNs)	Polypropylene sulfide-polyethylene glycol (PPS-PEG) and polypropylene sulfide-polyethylenimine (PPS-PEI). PPS provides ROS-response properties, PEG improves circulatory stability, and PEI endows particles with positive electrical properties to enhance glomerular targeting.	PPS-CPNs, especially CPN-10, showed good targeting and long retention in the kidney. The retention and accumulation of the nanoparticles in the glomeruli is further enhanced by binding to the negative charge of the glomerular basement membrane (GBM) via electrostatic interactions. Compared with highly charged particles, CPN-10 has reduced nonspecific distribution in the liver and lung, while reducing the potential toxicity.	Mouse	NIR fluorescence imaging/IHC	Intravenously injection (200 µg/kg, tail vein)
35574055 [ref. ⁸²]	2022	Weibo Cai	polyvinylpyrrolidone (PVP)-curcumin nanoparticles (PCurNP)	A series of povidone (PVP) -curcumin conjugates with different molecular weights (M10, M29, M40, representing average molecular weights of 10 kDa, 29 kDa, and 40 kDa, respectively) were designed and formed into nanoparticles (PCURnps). These NPS are formed through the hydrophobic interaction between PVP and curcumin, and their size can be modulated by the selection of PVP with different molecular weights.	Using positron emission tomography (PET) imaging technology, researchers observed the dynamic distribution and accumulation of PCurNP of different sizes in mice. PCurNP M10 showed the highest renal accumulation, whereas PCurNP M29 and PCurNP M40 showed relatively low renal accumulation	Mouse	PET	Intravenously injection (1mg, tail vein)
35394757 [ref. ⁸³]	2022	David Oupický	Polymeric plerixafor	Researchers have synthesized a series of Plerixafor-based polycationic polymers (PPs) and introduced different functional groups (such as hydroxyl, carboxyl, primary amine and alkyl groups) through copolymerization to adjust the charge and hydrophilicity of the polymers. The introduction of these functional groups affected the distribution of the polymer in vivo and the targeting of the kidney.	All synthesized polymers accumulate primarily in the damaged kidney or liver. In particular, polymers containing hydroxyl groups (PP-OH) have shown a tendency to selectively accumulate in damaged kidneys. The ratio of PP-OH(L) and PP-OH(H) was highest in the damaged kidney to liver, which was about 2.4-fold higher than PEI (polyethylene imine, a commonly used transfection reagent).	Mouse	IVIS Spectrum	Intravenously injection (2mg/kg, tail vein)

35880399 [ref: ⁶³]	2023	Danfei Chen	Polycaprolactone-polyethyleneimine nanoparticles (PCL-PEI)	To enhance renal drug distribution and cellular uptake by PGA-coated PCL-PEI. PGA is capable of receptor-ligand interaction with γ -glutamyl transpeptidase (GGT), which is highly expressed in the kidney, thus improving its targeting to the kidney	RGPP showed good circulation and renal targeting distribution in the DN mouse model, with a significant increase in the distribution of RGPP in the kidney and a decrease in the distribution of RGPP in the urine compared with RAPP, indicating that RGPP has a longer retention time in the kidney.	Mouse	IVIS Spectrum	Intravenously injection (5mg/kg, tail vein)
34931497 [ref: ⁸⁴]	2021	In-Kyu Park	Alternative copolymer (PS) of sorbitol and polyethyleneimine (PEI)	Developed a proximal renal tubule-targeting gene delivery system based on alternative copolymer (PS) of sorbitol and polyethyleneimine (PEI), modified with vimentin-specific chitobionic acid (CA), producing PS-conjugated CA (PSC) for targeting toward vimentin-expressing cells in the kidneys	Fluorescence signal showed that the fluorescence intensity of PSC-F675/pDNA complex in kidney was significantly higher than that in other organs such as liver, lung, spleen and heart. This suggests a high degree of renal targeting of this system	Mouse	IVIS Spectrum	Intravenously injection (1 μ g/kg, tail vein)
31534545 [ref: ⁸⁵]	2019	Pintong Huang	Polycaprolactone-polyethyleneimine (PCL-PEI)	Prepared kidney-targeted rhein (RH)-loaded liponanoparticles (KLPPR) with a yolk-shell structure composed by polycaprolactone-polyethyleneimine (PCL-PEI)-based cores and kidney targeting peptide (KTP)-modified lipid layers.	LPCCy5R was mainly distributed in the liver and lung, followed by the kidney and intestine. The fluorescence intensity of KLPPCy5R in the kidney is 2 to 4 times higher than that in the liver, lung, and intestine, and 7 to 20 times higher than that in the heart, spleen, and brain. The fluorescence intensity of KLPPCy5R was 2.6-fold higher in the kidney than that of LPCCy5R, indicating that KTP mediation could improve renal distribution and accumulation and decrease urinary excretion.	Mouse	IVIS spectrum	Intravenously injection (20mg/kg, tail vein)

(Continued)

Table I (Continued).

PMID	Year	Author	Carrier	Methods	Biodistribution	Model	Detection	Administration
28629080 [ref. ⁶²]	2017	Mohammad Ramezani	Polyethylenimine (PEI)	Modified polymyxin -PEI/DNA nanocomposites were prepared by binding PEI25 kDa or PEI10 kDa to polymyxin B via an amide reaction.	The accumulation of polymyxin B-modified nanoparticles in the kidney was increased compared with unmodified PEI/DNA nanoparticles, indicating that these nanoparticles were able to target the kidney efficiently.	Mouse	IVIS spectrum	Intravenously injection (60 µg, tail vein)
39236956 [ref. ⁸⁶]	2024	Heba Elmotasem	Spanlastics (SP) nanovesicles	Spanlastics (SP) nanovesicles were prepared using Span 60 and Labrasol or Brij35 as edge activators (EA). Cationic guar (CG) and hyaluronic acid (HA) were employed as coatings	Transdermal application of the modified formulation FRA-L-H-SP has enhanced therapeutic effect compared to the uncoated FRA-L-SP formula, and the free FRA transdermal delivery or the oral administration of the free FRA	Rat	Evaluation on the effect on blood glucose, insulin level, creatinine, and urea; investigation of kidney tissue	Transdermal application (5 mg/mL)
35803437 [ref. ⁸⁷]	2022	Genyang Cheng	Micelles & Chitosan	Use low molecular weight chitosan (CS) as a carrier, it can achieve targeted delivery by interacting with megalin receptors on the renal tubules. LU binds to citric anhydride (CA) to form ph-sensitive Lu-CA, which is then linked to CS via an amide bond to construct Lu-CA-CS. Cel is encapsulated in the hydrophobic core of the micelle and eventually forms the Cel@LU-CA-CS micelle.	IR780@LU-CA-CS micelles were rapidly enriched in the kidney after injection and peaked in fluorescence intensity at 12 hours. The fluorescence signal intensity of the kidney was significantly higher than that of other organs, indicating that the micelle had good kidney targeting. Compared with free IR780, the distribution concentration of nano-micelles in the kidney was increased by about 2-fold.	Mouse	NIR imaging	Intravenously injection (2mg/kg, tail vein)

41048153 [ref. ⁸⁸]	2025	Boaz Y. Bishop	Micelles	PEG-b-PPS block copolymers synthesized via anionic ring-opening polymerization, self-assembled into micelles via thin-film hydration. Lipid-anchored peptide amphiphiles (CLPVASC & CYNTTTHRC) incorporated at specified molar ratios, purified via Sephadex LH-20 column.	Dual-targeted micelles exhibited significantly increased accumulation in the injured kidney (3.4-fold higher than contralateral kidney; 67% higher than non-targeted micelles), while off-target distribution to liver, lung, spleen, and heart was markedly reduced (2.3-fold lower in lungs compared to injured kidney). Ex vivo IVIS imaging confirmed selective renal localization and reduced systemic dispersion.	Mouse	IVIS Spectrum	Intravenous injection via the retro-orbital plexus (75 μ L)
38652072 [ref. ⁸⁹]	2024	Eun Ji Chung	Micelles	Incorporate the basolateral targeting peptide GRGDSP (RGD) into previously reported drug carrier system called peptide amphiphile micelles (PAMs)	Via tail vein injection of RGD micelles, it was found that their accumulation in the kidney was significantly higher than that of untargeted micelles, and this accumulation was significantly reduced after inhibition of renal secretion	Mouse	IVIS Spectrum (ex vivo imaging)	IV (intravenously injection of vein) and IP (Intraperitoneal injection) (100 μ L, 1mM)
37394108 [ref. ⁹⁰]	2023	Chunjing Guo	Micelles	Novel hybrid micelles loaded Puerarin (Pue) based on Angelica sinensis polysaccharides (ASP) and Astragalus polysaccharide (APS) were fabricated with pH-responsive ASP-hydrazone-ibuprofen (BF) materials (ASP-HZ-BF, SHB) and sialic acid (SA) modified APS-hydrazone-ibuprofen materials (SA/APS-HZ-BF, SPHB)	SPSB@Dir micelles showed higher fluorescence intensity and more effective accumulation in the kidney site after injection compared with free DiR.	Mouse	Ex vivo fluorescence imaging	Intravenous injection (tail vein)
35872158 [ref. ⁹¹]	2022	Genyang Cheng	Micelles (Pluronic F127)	Folic acid-targeted pluronic F127 micelles (Cur/Res@FA-F127/TPGS) was designed to co-load the anti-inflammatory and antioxidant traditional Chinese medicine monomers curcumin (Cur) and resveratrol (Res).	The IR780@FA-F127/TPGS nanosystem showed a stronger fluorescence signal in the kidney than the unlabeled IR780, indicating that this system is able to reach HK-2 cells via folate receptor-mediated endocytosis.	Mouse	IVIS Spectrum	Intravenously injection (0.5mg/kg, tail vein)

(Continued)

Table I (Continued).

PMID	Year	Author	Carrier	Methods	Biodistribution	Model	Detection	Administration
33865397 [ref: ⁹²]	2021	Chang Seong Kim	Micelles	Hydrophobically modified glycol chitosan (HGC) nanomicelles loaded with tacrolimus (TAC) (HGC-TAC)	The fluorescence intensity from the kidneys was the most intense compared to those from other organs after injection of HGC-F675 nanomicelles	Mouse	In vivo fluorescence imaging	Intravenous injection (0.5 mg/kg)
34352625 [ref: ¹²]	2021	Zongning Yin	Micelles	Construct four-arm star polymers conjugated with a novel linear RWrNM peptide. And poly ϵ -caprolactone (PCL) hydrophobic core and brush poly (2-hydroxyethyl methacrylate) (PHEMA) hydrophilic shell were synthesized by ROP and SET LRP polymerization.	After tail vein injection of Dexam-4sPC21H21C/R2 micelles, the investigators observed a significant targeting effect of these micelles in the kidney. Compared with the unmodified 4sPC21H21C micelles, the micelles modified with RWrNM peptide accumulated more in the kidney.	Rat	IVIS Spectrum	Intravenously injection (50 μ g/kg, tail vein)
33253922 [ref: ⁹³]	2020	Jiansong Ji	Micelles	Kidney-targeted octenyl succinic anhydride- grafted fucoidan loaded with Cur (OSA-Fucoidan/Cur) was fabricated for synergistic treatment of AKI.	The near-infrared dye ICG labeled OSA-Fucoidan micelles (OSA-Fucoidan/ICG) were used to evaluate the renal targeting ability. The results showed that the fluorescence intensity of OSA-Fucoidan/ICG was significantly enhanced in the kidneys of LPS-induced AKI model mice compared with normal mice, indicating the excellent kidney-specific targeting ability of OSA-Fucoidan micelles during AKI treatment.	Mouse	IVIS Spectrum	Intravenously injection (/, tail vein)
33184578 [ref: ¹⁸]	2020	Eun JI CHUNG	Micelles	A KNP/MN patch was developed by incorporating folate-conjugated micelle nanoparticles into polyvinyl alcohol MN patches.	In the C57BL/6 mouse model, KNP was observed to accumulate mainly in the kidney, liver, intestine, and skin by in vitro imaging after percutaneous application of KNP/MN patches. KNP accumulation in the kidney was on average 2.2-fold higher at 24 hours and 7.7-fold higher at 48 hours after administration compared with non-targeted nanoparticles (NPS).	Mouse	IVIS Spectrum	Transdermal microneedles (KNP/MN)

33175576 [ref: ⁹⁴]	2020	Lejun Li	Micelles	Prepare chrysophanol-loaded micelles (CLM) to improve the oral bioavailability, targetability, and the preparation of CLM was achieved via thin-film dispersion technique.	Tissue distribution studies performed in mice revealed that CLM was rapidly distributed into the systemic circulation after administration. In contrast to free CH, CLM accumulated mainly in the liver and brain, while lower concentrations were found in the heart and lungs. This suggests that CLM is able to target the liver and brain efficiently.	Mouse	IHC	Oral administration (50mg/kg)
33005739 [ref: ⁵⁰]	2020	Yi Huang	Micelles	Peptide amphiphile micelles (PAM) functionalized with the zwitterionic peptide ligand, (KKEEE)3K	All micelles accumulated in the kidneys to a greater extent than all other organs with the exception of 90% PEG5000-(KKEEE)3K	Mouse	Ex vivo imaging	Intravenous injection
33405591 [ref: ²⁵]	2019	Jianqiang Hu	Micelles (Pluronic F127/P123)	Developed folate (FA)-modified Pluronic F127/P123 nanoparticles (FPNPs).	Researchers found that the fluorescence intensity of the kidney was much higher than that of other organs, indicating the kidney targeting ability of FPNPs. The accumulation of FPNPs in the kidney reached a maximum at 12 hours after injection, and a strong fluorescence signal was still observed up to 48 hours, demonstrating the long-term retention of FPNPs in the kidney.	Mouse	IVIS spectrum	Intravenously injection (0.5mg/kg, tail vein)
41390419 [ref: ⁹⁵]	2025	Zheng Xiao	PEGylated hollow polydopamine (HPDA)	A hollow polydopamine (HPDA) nanoshell was first synthesized by silica-templated polymerization and HF etching. Rosiglitazone was loaded into the cavity, then the surface was PEGylated (NH ₂ -PEG-NH ₂) and finally conjugated with the renal tubule targeting K3 peptide via EDC/NHS chemistry to yield Rosi@HPDA-PEG-K3 nanoparticles.	Cy5.5-labeled Rosi@HPDA-PEG-K3 i showed rapid liver uptake at 2 h, but kidney fluorescence surpassed liver by 24 h and remained high through day 7; K3 modification doubled renal accumulation versus non-targeted HPDA, with fibrotic kidney > contralateral kidney.	Mouse	IVIS Spectrum	Intravenously injection (10mg/kg, tail vein)

in the kidneys, there are prominent examples.^{75,77,78} However, it is important to note that the strong cationic charge of chitosan and similar polymers can also lead to dose-dependent cytotoxicity and nonspecific interactions with plasma components, a challenge that underscores the need for careful design and charge modulation.⁷⁷ To mitigate these issues and improve performance, various modifications have been developed. Modifications such as PEGylation (PCS) improved oral delivery and renal targeting of salvianolic acid B while potentially moderating surface charge.⁷⁹ Cationic chitosan-based nanoparticles (COS-SA) also demonstrated good renal targeting, which was maintained even after adsorption of a human serum albumin (HSA) corona.⁷⁴ Functionalized chitosan, like α -cyclam-p-toluic acid-conjugated chitosan (C-CS), can target the CXCR4 receptor overexpressed in injured kidneys.⁷⁶ Other cationic systems include poly-L-lysine (PLL) modified with L-serine, which achieved remarkable kidney-specific accumulation for potential radionuclide therapy,^{53,62} and polyethylenimine (PEI) derivatives.⁸⁴ Cationic polymeric nanoparticles designed with polypropylene sulfide-polyethylenimine (PPS-PEI) cores and PEG shells combine reactive oxygen species (ROS)-responsiveness with a tuned positive charge for enhanced glomerular targeting.⁸¹

Micelles

Micelles, formed from amphiphiles like Pluronic, do well in solubilizing hydrophobic drugs. Their small size favors renal distribution. Kidney-targeting efficiency is evidenced in studies using chitosan-based,^{87,92} polysaccharide-based,^{90,93} or peptide-amphiphile micelles^{50,88,89} while surface modification with ligands like folate^{25,91} or specific peptides¹² can significantly improve the targeting. Beyond intravenous administration, micellar systems have been successfully engineered for alternative routes. Oral formulations, such as kidney-targeted micelles protected within chitosan particles, can survive the gastrointestinal tract and subsequently accumulate in the kidneys, demonstrating the feasibility of non-invasive systemic delivery.⁸⁹ Similarly, transdermal micelle-loaded patches offer a potential route for sustained renal drug delivery.^{18,94}

Innovative Polymeric Constructs

These include polymeric plerixafor-based polycations (PPs) that target CXCR4,⁸³ polyvinylpyrrolidone-curcumin nanoparticles (PCurNPs) whose renal accumulation is influenced by polymer molecular weight,⁸² polycaprolactone-polyethylenimine (PCL-PEI) NPs coated with poly- γ -glutamic acid (PGA) for GGT-mediated renal targeting in diabetic nephropathy,^{63,85} polymeric nanoplexes (NPX) formed by electrostatic interaction for peptide delivery,⁸⁰ Poly(ethylene glycol)-polytyrosine nanocomplexes which have demonstrated passive yet significant kidney targeting and prolonged retention.⁹⁶ Hollow polydopamine nanoshells loaded with drugs, PEGylated, and conjugated with renal tubule-targeting peptides represent another innovative platform showing enhanced renal accumulation.⁹⁵

Lipid-Based Nanocarriers

Lipid-based nanocarriers, prized for their biocompatibility and various drug-loading, are important for kidney-targeting drug delivery. This class mainly includes liposomes, micelles and solid-core lipid nanoparticles (LNPs), each offering unique advantages for navigating renal physiology. Key studies are summarized in [Table 2](#).

Liposome

Liposomes encapsulate drugs in their aqueous core or lipid bilayers. Studies demonstrate their kidney accumulation potential, often enhanced by PEGylation to prolong circulation.^{98,99} Functionalization can further direct them, such as peptide-conjugated^{31,103} or sugar/HA-coated variants.¹⁰¹ Recent advancements include the development of ultrasound-responsive liposomes modified with L-serine (LIPs-S@TAK/PFP), which show strong kidney-specific accumulation and prolonged retention.⁹⁷ Hybrid systems like liposome-nanoparticle hybrids (LNHy), combining a lipid shell with PLGA or gold cores, also show effective renal targeting.¹⁰⁵

Lipid Nanoparticles (LNPs)

Lipid Nanoparticles (LNPs) represent a distinct type, primarily recognized for nucleic acid delivery. Unlike the aqueous-core, bilayer structure of liposomes, LNPs feature a solid, non-aqueous core composed of a lipid mixture. This structure is highly effective for encapsulating hydrophobic small molecules, as indicated by Phospholipid lipid nanoparticles (PLNs) achieving sustained renal accumulation of drugs.³¹ A key conceptual innovation is the Selective Organ Targeting

Table 2 Lipid-Based Nanocarriers

PMID	Year	Author	Carrier	Methods	Biodistribution	Model	Detection	Administration
41481962 [ref: ⁹⁷]	2026	Yingnan Guo	Liposome	LIPs-S@TAK/PFP is constructed by synthesizing a DSPE-PEG-S conjugate through covalent linkage of t L-serine to DSPE-PEG-COOH. This conjugate is then mixed with lipids. And then emulsified with perfluoropentane as a phase-change agent.	The nanoparticles (LIPs-S@TAK/PFP) exhibit strong kidney-specific accumulation with minimal distribution to other major organs (heart, liver, spleen, lungs). Targeted delivery is enhanced by L-serine modification, enabling prolonged renal retention and reduced systemic exposure.	Rat	IF&IHC	Intravenously injection (10mg/kg, tail vein)
38371457 [ref: ⁹⁸]	2024	Wei Xiao	Liposome	Briefly, soybean lecithin, ATS, TPP, cholesterol, and DSPE-MPEG2000 were dissolved in dichloromethane and the solution was dried using rotary evaporation, then proper amount of water was added into the bottle for hydration to obtain the liposomes solution. Ultrasound the solution for 3 min to generate T-A-Ls.	T-A-Ls in the kidney tissue of AKI mice was significantly increased compared with that of healthy kidneys, the concentration in the heart, liver, spleen, and lung tissue samples of the AKI model mice was not increased compared with the control animals.	Mouse	IVIS Spectrum	Intravenously injection (30mg/kg, tail vein)
38537579 [ref: ⁹⁹]	2024	Carlos Lopez-Larrea	Liposome	Liposomes efficiently encapsulated JQ1 in both the membrane and core	JQ1-NPs reached the kidney within 1 h after injection and maintained a high level of accumulation in the kidney over the next 24 h	Mouse	IVIS Spectrum	Intravenously injection (40mg/kg, tail vein)
38973655 [ref: ¹⁰⁰]	2024	Daniel J. Siegwart	Lipid nanoparticles	SORT LNPs were formulated with different lipid combinations to optimize their targeting ability to the kidney, 18 Phosphatidic acid (PA)-15, as a colipid, has been shown to be critical for achieving renal distribution. The concentration ratio of PA as well as the surface charge of the nanoparticles were adjusted in the formulation to enhance their targeting to renal tubules and endothelial cells.	When the lipid formulation 18PA-15, with phosphatidic acid as a key component, was used, the distribution of LNPs to the kidney was approximately 13%, which was significantly higher than other conventional LNPs	Mouse	IVIS Spectrum	Intravenously injection (0.5–1mg/kg, tail vein)
36442556 [ref: ¹⁰¹]	2022	Shufang Wang	Hyaluronic acid-coated liposome (HALP)	HALP is formed by self-assembly of hyaluronic acid (HA) through the electrostatic interaction with curcumin-loaded cationic liposomes (LP)	The accumulation of HALP was greater in damaged kidneys compared to normal kidneys, indicating better targeting of HALP	Mouse	IVIS Spectrum	Intravenously injection (200 μL, tail vein)

(Continued)

Table 2 (Continued).

PMID	Year	Author	Carrier	Methods	Biodistribution	Model	Detection	Administration
34968038 [ref: ¹⁰²]	2022	Zhixiang Yuan	Liposome-nanoparticle hybrids (Au-LNHy)	Liposome-nanoparticle hybrids (Au-LNHy) were formed by coating the surface of gold nanoparticles with a phospholipid bilayer; the Au-LNHys formed were comodified with PEG and $\alpha 8$ integrin antibodies to obtain gold nanoparticle immunoliposomes (Au-ILs). Next, the Au-ILs were loaded with dexamethasone and TGF β 1 siRNA to obtain DXMS/siRNA@Au-ILs.	The fluorescence intensity of targeted-modified Au-ILs in the kidneys was significantly higher than in other organs, demonstrating renal targeting specificity.	Mouse	IVIS Spectrum	Intravenously injection (1.5mg/kg, tail vein)
31931051 [ref: ¹⁰³]	2020	Jianhan He	Liposome	The pentapeptide CREKA, which specifically binds fibronectin, was conjugated to PEGylated liposomes (CREKA-Lip).	The results showed a significant increase in the accumulation of CREKA-Lip in the fibrotic kidney at 4 h after administration of CREKA-Lip compared to control (Lip), indicating that CREKA-Lip is able to specifically target the fibrotic kidney.	Mouse	IVIS spectrum	Intravenously injection (1mg/kg, tail vein)
34925707 [ref: ³¹]	2021	Ling Zhang	Phospholipid lipid nanoparticles (PLNs)	The researchers designed a targeted delivery system called peptides coupled CLT-phospholipid lipid nanoparticles (PC-PLNs), which took advantage of the unique structural and pathological characteristics of glomeruli by optimizing the surface charge and size of the nanoparticles. This system can efficiently deliver CLT to damaged glomerular endothelial cells and podocytes.	The accumulation of HPos-D-PLNs in the kidney was significantly higher than in the other three groups	Mouse	IVIS Spectrum	Intravenously injection (100 μ g/kg, tail vein)
35750132 [ref: ⁴⁹]	2022	Anna Schwendeman	High-density lipoprotein (sHDL) nanodiscs	sHDL nanodiscs, consisting of phospholipids and ApoA-I mimetic peptides, have an ultra-small size (10–15 nm), a hydrophobic core for loading hydrophobic drugs, ease of modification, a long cycling half-life (12–24 hours), and clinical safety.	Fluorescence intensity was quantified in the major organs of control sHDL/diR- and KT-sHDL/diR-treated mice: heart, liver, spleen, lung, kidney, and intestine. The results showed that the fluorescence intensity in the kidneys of KT-sHDL/diR-treated mice was almost 3-fold higher than that of sHDL/ DiR-treated mice.	Mouse	IVIS Spectrum	Intravenously injection (1.5mg/kg, tail vein)

39236956 [ref. ⁸⁶]	2024	Heba Elmotasem	Spanlastics (SP) nanovesicles	Spanlastics (SP) nanovesicles were prepared using Span 60 and Labrasol or Brij35 as edge activators (EA). Cationic guar (CG) and hyaluronic acid (HA) were employed as coatings	Transdermal application of the modified formulation FRA-L-H-SP has enhanced therapeutic effect compared to the uncoated FRA-L-SP formula, and the free FRA transdermal delivery or the oral administration of the free FRA	Rat	Evaluation on the effect on blood glucose, insulin level, creatinine, and urea; investigation of kidney tissue	Transdermal application
41475473 [ref. ¹⁰⁴]	2026	Chunjuan Xia	Nanobubbles (NBs)	NBs(SDF-1) were synthesized by conjugating biotinylated SDF-1 chemokine onto streptavidin-coated nanobubbles (NBs) via biotin-streptavidin linkage, The resulting NBs(SDF-1) were then co-cultured with GFP-expressing mesenchymal stem cells (MSCs) to generate the final therapeutic complex: NBs(SDF-1)-MSCs.	The primary biodistribution target of the NBs(SDF-1)-MSCs complex is the kidneys . In vivo tracking demonstrated specific accumulation and retention of the labeled cells in the kidneys for up to 7 days , with significantly enhanced homing efficiency under ultrasound-mediated microbubble destruction (UTMD).	Rat	IVIS Spectrum	Intravenously injection (100 μ L, tail vein)

(SORT) platform. By systematically varying lipid composition, for instance, incorporating specific “SORT” lipids like phosphatidic acid (PA), these LNPs can be intrinsically “programmed” to achieve preferential distribution to different organs, including the kidneys, thereby enabling organ-specific delivery through lipid design itself rather than mandatory surface conjugation.¹⁰⁰

Other Specialized Lipid Systems

High-density lipoprotein (HDL) nanodiscs are synthetic, discoidal particles (10–15 nm) composed of phospholipids and apolipoprotein A-I mimetic peptides. Their ultrasmall, flat morphology is important for renal filtration. When further functionalized with kidney-targeting peptides (KTPs), these nanodiscs (KT-sHDL) demonstrated nearly 3-fold higher renal accumulation.⁴⁹ Spanlastic nanovesicles, formed using non-ionic surfactants and edge activators. Their elastic nature is particularly suited for non-invasive administration routes. For instance, transdermal spanlastic coated with cationic guar gum and hyaluronic acid have shown promise for renal-targeted therapy, offering a potential alternative to systemic injections.⁸⁶ Nanobubbles (NBs) conjugated with targeting ligands can also serve as carriers to enhance the homing and retention of therapeutic cells like mesenchymal stem cells (MSCs) to the kidneys, especially when combined with ultrasound.¹⁰⁴

Inorganic and Hybrid Nanoparticles

Inorganic and hybrid nanoparticles have unique physicochemical properties, such as optical characteristics for imaging, catalytic activity, and robust structures for controlled drug release, making them very useful for kidney-targeted delivery. Some Key systems are summarized in Table 3.

Gold Nanoparticles (AuNPs)

Gold nanoparticles (AuNPs), especially when modified with biocompatible ligands like glutathione (GSH), show favorable kidney-targeting. Studies have shown that GSH-modified AuNPs rapidly accumulate in the kidneys within 1–2 hours post administration and can be efficiently excreted via urine, with a distribution profile favoring the kidneys not the liver.^{61,111} Rapid renal uptake and great ability of self-assembling into drug-loaded platforms make AuNPs effective therapy for conditions like acute kidney injury (AKI).¹¹⁰ Further modifications, such as coating with PEG and phenolic compounds constructed PEGylated and phenol-enriched Au nanorods (Au-M NRs) that show enhanced and prolonged accumulation in the renal cortex of injured kidneys.¹⁰⁹

Ultrasmall Carbon-Based Nanomaterials

PEGylated reactive carbon dots (P-RCDs) with diameters around 5–8 nm are innovative “theranostic” platform. Their sub 10 nm size make it easy for passaging through the glomerular filtration barrier, leading to significant and prolonged renal accumulation.¹¹² Selenium-doped carbon dots (Zt-SeCDs) further expand this category, showing rapid renal accumulation and clearance, with significantly higher signals in injured kidneys.¹⁰⁶ Hyaluronic acid-conjugated reduced graphene oxide nanoparticles (HA/rGO) represent another carbon-based platform that can be loaded with hydrophobic drugs and shows specific accumulation in injured kidneys over time.¹⁰⁸

Silica-Based Nanocarriers

Silica-based nanocarriers include mesoporous silica (mSiO₂) and silica-cross-linked micelles (SCLMs), they provide high stability and versatile surface chemistry for functionalization. Kidney targeting can be significantly enhanced by surface modification with LTH peptide, resulting in increased kidney accumulation and reduced off-target distribution in the liver and spleen.²⁶ Furthermore, SCLMs of specific sizes have demonstrated a remarkable ability to selectively accumulate in damaged renal tubules with extended residence times of up to 10 days, highlighting their potential for sustained, pathology-specific drug delivery.¹¹³

Hybrid Systems

MOFs (Metal–Organic Framework) offers ultrahigh drug loading, tunable pore size, and easy surface functionalization for targeted delivery, for instance, zeolite imidazolate framework-8 (ZIF-8) nanoparticles coated with renal tubular

Table 3 Inorganic and Hybrid Nanoparticles

PMID	Year	Author	Carrier	Methods	Biodistribution	Model	Detection	Administration
40315398 [ref: ¹⁰⁶]	2025	Man Li	Selenium-doped carbon dots (Zt-SeCDs)	Zt-SeCDs were synthesized by one-pot hydrothermal carbonization, selenourea and o-phenylenediamine were first reacted to form Se-doped carbon dots (SeCDs); Zileuton was then covalently linked to the surface amino groups of SeCDs via an ROS-cleavable TK-NHS linker.	Zt-SeCDs rapidly accumulate in the kidneys, peaking at 12 h and clearing by 48 h; Fluorescence in AKI kidneys is 6-fold higher than in healthy ones, while off-target signals in liver, spleen, and lung remain low.	Mouse	IVIS Spectrum	Intravenously injection (5mg/kg, tail vein)
41344845 [ref: ¹⁰⁷]	2025	Hanshu Sun	Gallium Nanodroplets	Gallium nanodroplets (Ga NDs) are synthesized by ultrasonication of liquid gallium in water for 10–30 minutes, forming capsule-like particles with a GaOOH/Ga ₂ O ₃ shell and a liquid Ga core.	Ga NDs showed preferential renal accumulation after intravenous injection, with significant kidney targeting and rapid urinary excretion, and exhibit enhanced retention in injured kidneys without major systemic distribution.	Mouse	IVIS Spectrum	Intravenously injection (20mg/kg, tail vein)
41346711 [ref: ¹⁰⁸]	2026	Seungjun Lee	Hyaluronic acid-conjugated reduced graphene oxide nanoparticles (HA/rGO)	The system is constructed by synthesizing HA-conjugated reduced graphene oxide nanoparticles through in-situ reduction of graphene oxide in a hyaluronic acid solution using ascorbic acid and high-power sonication. The hydrophobic anti-fibrotic drug paricalcitol is then loaded onto HA/rGO via hydrophobic interactions.	Significant accumulation occurs specifically in the injured kidney, with peak fluorescence signal observed at 48 hours post-injection. No distinct renal accumulation is detected at 24 hours. The nanoparticles show minimal uptake in contralateral kidneys and extrarenal organs such as brain, spleen, heart, lung, and liver under physiological conditions, though some increased signals in these organs post-IR injury are attributed to reduced systemic clearance.	Mouse	IVIS Spectrum	Intravenously injection (0.32mg/kg, tail vein)
40763583 [ref: ¹⁰⁹]	2025	Chunyan Fang	Gold nanorods (Au NRs)	Au-M nanorods are gold nanorods surface-coated with thiolated PEG2000-amine and then covalently linked to ring-opened 5,8-dihydroxypsoralen, yielding a PEGylated, phenol-enriched.	Au-M nanorods rapidly accumulate in the renal cortex of AKI mice, reaching three times the level seen in healthy kidneys, and remain there for >48 h with minimal retention in liver or spleen.	Mouse	ICP-MS	Intravenously injection (40mg/kg, tail vein)
39423345 [ref: ¹¹⁰]	2024	Yingyu Huang	Gold nanoparticle (AuLA)	Glutathione-coated, near-infrared emitting gold nanoparticles	The kidney fluorescence intensity in rhabdomyolysis-induced AKI was ~8.4 times higher than that in the control group	Mouse	In vivo fluorescence imaging	Intravenous injection

(Continued)

Table 3 (Continued).

PMID	Year	Author	Carrier	Methods	Biodistribution	Model	Detection	Administration
32884257 [ref: ⁶¹]	2020	Shu bin Wang	Gold nanoparticle (AuLA)	A glutathione (GSH)-modified fluorescent gold nanoparticle termed AuLA-GSH was prepared and a Co ²⁺ -induced self-assembly drug delivery platform termed AuLA-GSH-Co was constructed.	Most of the AuLA- GSHs accumulated in the kidney and bladder at 1 h p.i., indicated that AuLA-GSH could specifically target the kidney and be excreted in urine, CI values indicated a remarkable advantage of AuLA-GSH in kidney targeting than liver.	Mouse	IVIS Spectrum	Intraperitoneally injection (5mg/kg/day) for 7days
30681674 [ref: ¹¹¹]	2019	Lishan Tan	Gold nanoparticle (AuLA)	Glutathione (GSH)-modified Au nanoparticles (GLAuNPs) and Co ²⁺ self-assemble into nanoassemblies (GLAuNPs-Co)	GLAuNPs-Cy7 and GLAuNPs-Co-Cy7 showed rapid kidney accumulation 1 h after administration compared with the Cy7 group, which was sustained for at least 12 h	Mouse	Fluorescence microscope	Transdermal application (100 mg/kg)
38764416 [ref: ¹¹²]	2024	Jinsong Ren	Ultrasmall nanocarbons (P-RCDs)	P-RCDs is derived from 3,4, 5-trihydroxystyrene and is prepared by a hydrothermal carbonization process. Pegylation of P-RCDs by interaction with mPEG-DSPE enhances its biocompatibility and cycling stability.	There was a significant accumulation of P-RCDs in the kidney, and a strong renal fluorescent signal was still detectable up to 72 h after injection, indicating high renal accumulation and long-term retention of P-RCDs in vivo.	Mouse	IVIS Spectrum (ex vivo)	Intravenously injection (5mg/mL, tail vein)
37121517 [ref: ⁴⁸]	2023	Xinze Li	Zeolite imidazolate framework-8 nanoparticles	Prepare the kidney targeting peptide-modified renal tubular epithelial cell membrane to coat zeolite imidazolate framework-8 nanoparticles for FGF21 delivery (KMZ@FGF21)	KMZ@FGF21 showed obvious renal fluorescence signal within 2 hours after injection, and its fluorescence signal in the kidney was stronger than that in the other groups. Compared with simple FGF21 and unencapsulated Z@FGF21, KMZ@FGF21 could significantly prolong the retention time of drug in the kidney, and still retain significant fluorescence signal within 24 hours. The distribution of KMZ@FGF21 in organs other than the kidney was significantly reduced, showing its higher renal targeting ability.	Mouse	IVIS Spectrum	Intravenously injection (0.5mg/kg, tail vein)

36786440 [ref: ¹¹³]	2023	Juanjuan Peng	Silica cross-linked micelles (SCLMs)	Chemical cross-linking with a silicon compound, such as silane, further enhances the stability of the micelles and avoids their dissociation in the blood circulation. atorvastatin, an antioxidant and anti-inflammatory drug, was loaded inside the micelles.	SCLMs labeled with fluorescent dye showed almost no accumulation in healthy renal tissue, whereas a significant fluorescent signal was shown in damaged renal tubules. The residence time of 13 nm SCLMs in damaged renal tissue can be up to 10 days, much longer than that of free dyes or particles of other sizes.	Mouse	IVIS Spectrum	Intravenously injection (5mg/kg, tail vein)
36719986 [ref: ²⁶]	2023	Zhiyu He	Porous silicon-based nanocarrier (mSiO ₂)	Use disulphide bond-rich mesoporous silicon (mSiO ₂) nanomaterials as the carrier, silanization modification (Mal-PEG-silane) and coupling of renal tubule-targeting peptide (LTHVVWL) were used to enhance the kidney targeting ability.	The fluorescence intensity of nanoparticles modified with the LTH targeting peptide was about 1.7-fold higher in the kidney than that of the unmodified group, indicating that the targeting peptide could significantly enhance the enrichment effect in the kidney. The fluorescence signal was significantly attenuated in the liver and spleen, indicating a reduction in untargeted distribution.	Mouse	NIR images	Intravenously injection (0.2mg/kg, tail vein)

epithelial cell membranes forming KMZ@FGF21 showed enhanced and prolonged kidney retention of FGF21 compared to unencapsulated controls, with reduced distribution to non-renal organs.⁴⁸ Gallium nanodroplets (Ga NDs), synthesized from liquid gallium, have shown preferential renal accumulation and rapid urinary excretion, with enhanced retention specifically in injured kidneys.¹⁰⁷

Bio-Derived & Biomimetic Carriers

Harnessing materials derived from natural biological systems inspire a powerful strategy for kidney-targeted delivery. These carriers can be engineered to mimic natural pathways or exploit specific biorecognition, thereby enhancing kidney specificity and reducing immunogenicity. This section categorizes them into protein and peptide-based systems, cell-mimetic and membrane-derived platforms, and other natural biomolecular carriers, with key examples summarized in Table 4.

Elastin-Like Polypeptides (ELPs)

Elastin-like Polypeptides (ELPs) are thermally responsive, biodegradable biopolymers composed of repeating pentapeptide sequences Val-Pro-Gly-X-Gly. Their modular design allows for precise fusion with therapeutic proteins and functional peptides. Conjugation of a kidney-targeting peptide (KTP) to the ELP has proven highly effective, redirecting biodistribution from the liver to the kidneys and achieving renal accumulation levels 5- to over 150-fold higher than untargeted ELP. This strategy significantly prolongs the half-life of therapeutic cargo in renal tissues and has demonstrated efficacy in models of chronic kidney disease.^{119–121} Recent work has optimized ELP constructs by varying the number of repeating units and amino acid composition to fine-tune renal accumulation, with some constructs showing highly selective and dose-dependent uptake in the renal cortex and proximal tubules.¹¹⁸

Serum Albumin and Derivatives

Cationic bovine serum albumin (cBSA) has a natural affinity of albumin for receptors highly expressed on renal tubular epithelial cells such as megalin and cubilin. CBSA can form stable nanocomplexes with nucleic acids via electrostatic interactions, facilitating targeted delivery to fibrotic kidneys and significantly enhancing renal accumulation compared to free therapeutics.¹²⁵ Low Molecular Weight Proteins (LMWPs) with their small size (< 30 kDa) and natural renal filtration are served as effective carriers to concentrate conjugated drugs within the kidney.¹²⁴

Extracellular Vesicle (EVs/Exosomes)

Extracellular Vesicles are endogenous nanovesicles that facilitate intercellular communication. Their membrane is endowed with a rich repertoire of adhesion proteins and receptors, conferring innate tropism for specific cell types. Engineered EVs loaded with therapeutic agents show precise localization to renal tubular epithelial cells, endothelial cells, and macrophages in injured kidneys. Physical methods like ultrasound-targeted microbubble destruction (UTMD) can further enhance their renal delivery efficiency.²¹ Recent innovations include the use of exosomes derived from mesenchymal stem cells (MSC-Exo) formulated into dissolving microneedle patches for direct, on-site renal application during surgery.¹¹⁵ Furthermore, extracellular vesicles isolated from commercial milk have been successfully loaded with siRNA via electroporation and, upon oral administration, show specific accumulation in injured proximal tubule cells, demonstrating the potential of oral EV-based delivery.¹¹⁷

Cell Membrane-Coated Nanoparticles

Cell Membrane-Coated Nanoparticles involve cloaking synthetic nanoparticle cores with natural cell membranes, creating biomimetic “camouflage.” Platelet membrane vesicles (PMVs), which express P-selectin glycoprotein ligand-1 (PSGL-1), can be coated onto PLGA nanoparticles. The resulting PMV@PLGA complex demonstrates significant and prolonged accumulation in damaged kidney areas over 72 hours by leveraging PSGL-1-mediated targeting to activated endothelium at injury sites.³² Similarly, nanoparticles coated with neutrophil-derived membranes utilize the same PSGL-1 mechanism for targeted delivery to injured renal endothelial cells.¹²² A sophisticated biomimetic system combines upconversion nanoparticles (UCNPs) encapsulated in thylakoid membranes and further cloaked with activated renal

Table 4 Bio-Derived & Biomimetic Carriers

PMID	Year	Author	Carrier	Methods	Biodistribution	Model	Detection	Administration
40934095 [ref: ¹¹⁴]	2025	Xiaojuan Hu	Thylakoid membrane and renal tubular epithelial cell membranes	The UCTR consists of thylakoid membrane (TM)-encapsulated UCNPs cloaked with activatedrenal tubular epithelial cell membranes (RECM)	Healthy kidneys clear the particles within 10 h, whereas AKI kidneys reach peak accumulation at 4 h with 6–7-fold higher fluorescence intensity; the signal co-localizes strongly with tubular markers AQP1/Cadherin-16, achieving disease-selective targeting.	Mouse	IVIS Spectrum	Intravenously injection (4mg/kg), 980 nm NIR-II laser, 0.4 W cm ⁻² , 5 min per kidney, applied 4 h post-injection and repeated every other day for 7 days.
39845407 [ref: ¹¹⁵]	2025	Samin Taghavi	Exosomes derived from mesenchymal stem cells (MSC-Exo)	Exosomes were mixed with methacrylated hyaluronic acid, cast into PDMS micromolds, UV-cross-linked to form dissolving microneedles, and backed with PVA to create a ready-to-apply patch.	On-site renal treatment without delivery	Mouse	/	The microneedle patch was applied directly onto the exposed renal capsule during surgery. (100 µg mL ⁻¹ MSC-derived exosomes, 3 µg/mouse).
40049024 [ref: ¹¹⁶]	2025	Yu Ren	DNA tetrahedral	Four DNA strands self-assemble into a 10 nm tetrahedral framework (tFNA). G-quadruplex DNA is then hybridized to its vertices and loaded with Hemin in K ⁺ buffer, yielding a 4.8 nm G4/Hemin-tFNA nanocage with peroxidase-like activity.	In healthy mice the 4.8 nm nanocage is rapidly filtered by the glomeruli and cleared within 2 h, whereas in AKI mice it is retained in renal tubules for ≥4 h, producing kidney-selective accumulation with minimal off-organ signal.	Mouse	IVIS Spectrum	Intravenously injection (4mg/kg)
41246803 [ref: ¹¹⁷]	2025	Hochung Jang	Extracellular Vesicle	The system is constructed by isolating extracellular vesicles from commercial milk through sequential centrifugation and filtration, followed by loading PTP1B-targeting siRNA into the vesicles via electroporation.	Following oral delivery, PTPi@mEVs accumulate mainly in the kidneys (peak at 9 h), specifically in injured proximal tubule cells, with minimal uptake by immune cells. Free siRNA shows no renal accumulation due to degradation.	Mouse	IVIS Spectrum	Oral administration (1mg/mouse)

(Continued)

Table 4 (Continued).

PMID	Year	Author	Carrier	Methods	Biodistribution	Model	Detection	Administration
41478668 [ref: ¹¹⁸]	2025	Adesanya A. Akinleye	ELP	The coding sequence for the MMP-2i peptide was fused in frame with the ELP coding sequence for expression in E. coli, to optimize the construct, 3 additional proteins were made using varying numbers of VPGxG repeats (63, 127, or 255) and an "x" residue of V, G, or A in a 1:4:3 ratio. The final constructs in this series were called ELP63-MMP-2i (25 kDa), ELP127-MMP-2i (50 kDa), and ELP255-MMP-2i (99 kDa).	The ELP-MMP-2i fusion protein shows highly selective and dose-dependent accumulation in the kidney, particularly in the renal cortex and proximal tubules, with minimal uptake in other major organs. Renal concentrations exceed the therapeutic IC50, supporting its potential as a kidney-targeted antifibrotic therapy.	Rat	IVIS Spectrum	Intravenously injection or Subcutaneous (600nmol/kg)
33130676 [ref: ¹¹⁹]	2020	Alejandro R. Chade	ELP	Designed a fusion of vascular endothelial growth factor (VEGF) conjugated to an elastin-like polypeptide (ELP) carrier protein with an N-terminal kidney-targeting peptide (KTP).	By using a kidney-targeting peptide (KTP), the investigators were able to increase VEGF deposition in the kidney and prolong its half-life in tissues, showing better kidney specificity compared to untargeted ELP constructs.	Pig	IHC	Intrarenal injection of renal (100µg/kg)
31635263 [ref: ¹²⁰]	2019	Gene L. Bidwell III	ELP	Elastin-like polypeptides (ELP) are versatile protein biopolymers used in drug delivery due to their modular nature. The ELP-VEGF fusion protein was modified by adding a kidney-targeting peptide (KTP) to the N-terminus.	Addition of KTP slowed the rate of ELP clearance in vivo and increased its deposition in the kidney. In addition, the addition of KTP redirected ELP-VEGF, which was originally found in high concentrations in the liver, to the kidney.	SKH-1 Elite hairless mice	IVIS spectrum	Intravenously injection (20mg/kg, femoral vein)
27784692 [ref: ¹²¹]	2016	Alejandro R. Chade	ELP	Modified ELP at its NH2-terminus with KTP and at its COOH-terminus with a cysteine residue for tracer conjugation	Accumulated in kidneys at levels fivefold higher than untargeted ELP, showing renal levels 15- to over 150-fold higher than in other major organs	Rat and swine	IVIS Spectrum	Intravenously injection (100 mg/kg, femoral vein)
38782155 [ref: ³²]	2024	Xinzhong Huang	Platelet membranes (PMVs)	Platelet membranes (PMVs) and polylactic-co-glycolic acid (PLGA) nanoparticles were used to prepare PMVs @PLGA complex, which was combined with TGF-β1 siRNA to form PMVs @TGF-β1-siRNA NP complex.	In vivo and ex vivo imaging indicated the fluorescence intensity in the area of the damaged kidney increased significantly within 72 h, indicating that the PMVs@PLGA complex accumulated in the area of the damaged kidney.	Mouse	IVIS Spectrum	Intravenously injection 20 µg, tail vein)

38631490 [ref: ¹²²]	2024	Ruipeng Jia	Neutrophil- derived nanovesicles	Use a Layer-by-Layer (LbL) self-assembly technique, IL-37 was encapsulated in neutrophil membrane-derived nanovesicles (N-MVs) to form N-MV@IL-37. P-selectin glycoprotein ligand-1 (PSGL-1) was used as a targeting molecule to enhance the targeting ability of N-MVs to the injured kidney by binding to the neutrophil membrane	In vivo and in vitro analysis indicated that N-MVs and N-MV@IL-37 can specifically target damaged renal endothelial cells, and this targeting ability can be achieved through a PSGL-1-mediated mechanism	Rat	IVIS Spectrum (ex vivo imaging) and IF	Intravenously injection (200 µg, tail vein)
35643195 [ref: ¹²³]	2022	Ruiping Zhang	Melanin nanoparticles	The investigators used melanin nanoparticles (MNPS) as drug carriers, loaded with the PARP-1 inhibitor PJ34, and conjugated anti-GPR97 antibody to the surface of MNPS via EDC/NHS reaction to form GMP NPS.	PA imaging results showed that the PA signal in the mouse kidney gradually enhanced over time and peaked after 6 h of GMP nanoparticle administration, suggesting targeted accumulation of GMP nanoparticles in the kidney. After 24 h, the major organs of mice (heart, liver, spleen, lung, and kidney) were imaged by PA imaging to determine the distribution of GMP nanoparticles in these organs. The results showed that GMP nanoparticles were mainly distributed in the liver and spleen, and only a small amount accumulated in the kidney.	Mouse	Vevo LAZR- X PA imaging system	Intravenously injection (3mg/ mL, 200µL, tail vein)
9407519 [ref: ¹²⁴]	1997	Marijke Haas	Low- molecule- weight protein (LMWP)	Low-molecule-weight protein (LMWP) carrying renal specific targeting (NSAID) naproxen	The naproxen concentrates on the mice kidney	Rat	In vivo radiolabeled imaging	Intraperitoneal injection (60mg/kg)

(Continued)

Table 4 (Continued).

PMID	Year	Author	Carrier	Methods	Biodistribution	Model	Detection	Administration
34087588 [ref: ¹²⁵]	2021	Yao Fu	Cationic bovine serum albumin (cBSA)	Cationic bovine serum albumin (cBSA) was used to compound with miR-29b to form nanocomposites (cBSA/miR-29b) through electrostatic interaction. Four-arm star polymers of poly (ϵ -caprolactone) (PCL) hydrophobic core and brush poly (2-hydroxyethyl methacrylate) (PHEMA) hydrophilic shell were synthesized by RAFT and SET LRP polymerization reactions. Loading cBSA/miR-29b nanocomposites into host-guest hydrogels forms a hybrid platform system to achieve prolonged release of therapeutic nucleic acids to alleviate or reverse renal fibrosis.	The renal targeting efficacy of cBSA/miR-29b nanocomposite and F127-HA hydrogel was evaluated in a mouse model of unilateral ureteral obstruction (UUO). It was found that the accumulation of cBSA/miR-29b nanocomplexes was significantly increased in the kidney compared to the free miR-29b solution	Mouse	IVIS Spectrum	Intravenously injection (100 μ g/kg, tail vein)
32851154 [ref: ²¹]	2020	Bi-Cheng Liu	Extracellular vesicle	EVs are small membrane-structured particles secreted by cells. The membrane surface of EVs contains a variety of proteins and receptors, which enable them to interact with specific cells or tissues to achieve targeted delivery. Ultrasound-assisted microbubble destruction (UTMD) technology can be used to increase the permeability of EVs in the kidney and further improve the efficiency of drug delivery.	IL-10+ EVs were mainly localized in renal tubular epithelial cells, endothelial cells and macrophages in the kidney. In particular, more IL-10+ EVs were internalized in proximal convoluted tubule cells than in distal convoluted tubule cells, which may be because proximal convoluted tubule cells are more sensitive to ischemic injury.	Mouse	IVIS Spectrum	Intravenously injection (200 μ g/kg, tail vein)

32169456 [ref: ¹²⁶]	2020	Lujiang Yuan	Inulin	Clarify the potential of IN as an efficient renal-specific drug carrier by synthesizing the new IN-FeA and IN-EDA-FeA conjugates	Inulin and its conjugates, such as IN-FEA and IN-EDA-FEA, show clear renal targeting IN vivo. This suggests that these conjugates are able to efficiently deliver drugs to the kidney through the blood circulation system. FeA accumulation IN other organs such as heart, liver, spleen, lung, and brain was significantly reduced IN in-FEA and In-EDA-FEA compared to free FeA, suggesting that the conjugate was able to reduce drug distribution in non-target organs.	Mouse	HPLC	Intravenously injection (200mg/kg, tail vein)
41189670 [ref: ¹²⁷]	2025	Yinghan Wang	Fucoidan (Fu)	Fu-4-PBA/Po NPs are self-assembled, dual-targeting nanoparticles formed by conjugating fucoidan with 4-PBA and encapsulating polydatin, enabling P-selectin-mediated inflammation targeting and ER-specific delivery	In vivo imaging and pharmacokinetic studies showed that orally administered Fu-4-PBA/DIR nanoparticles accumulated predominantly in the kidneys, indicating renal targeting potential. The nanoparticles significantly improved the oral bioavailability of polydatin, achieving a 2.2-fold higher peak concentration and a 2-fold increase in AUC compared to free drug. Tissue distribution analysis confirmed elevated drug levels in both the liver and kidneys, with the nanoformulation demonstrating sustained release and reduced systemic dispersion compared to the rapid clearance of free dye.	Mouse	IVIS Spectrum	Oral administration (100mg/kg)

tubular epithelial cell membranes (RECM). This dual-membrane “UCTR” platform achieves highly disease-selective targeting to injured renal tubules, with minimal uptake in healthy kidneys.¹¹⁴

Melanin Nanoparticles (MNPs)

Melanin Nanoparticles (MNPs) are derived from the natural pigment melanin, known for its biocompatibility, biodegradability, and strong antioxidant properties. They also serve as excellent photoacoustic (PA) imaging agents. When functionalized with targeting ligands, they can achieve targeted accumulation in the kidney, allowing for simultaneous therapy and imaging, although significant distribution to the reticuloendothelial system like liver and spleen may still occur.¹²³

Natural Polysaccharides and Conjugates

Inulin (IN) is a natural, water-soluble polysaccharide generally recognized as safe material. Due to its small hydrodynamic diameter, it is readily filtered by the kidneys. Conjugation of drug molecules to inulin such as IN-FeA or IN-EDA-FeA creates kidney specific prodrugs that significantly enhance drug delivery to the kidneys while markedly reducing off-target distribution in other major organs.¹²⁶ Fucoidan, a sulfated polysaccharide, has been exploited for its P-selectin targeting ability. Self-assembled nanoparticles based on fucoidan conjugated with 4-PBA show dual-targeting, upon oral administration, achieve predominant accumulation in the kidneys, improving oral bioavailability and enabling kidney targeted therapy.¹²⁷

DNA Tetrahedral

DNA-based nanomaterials offer precise structural control for renal targeting. Ren et al designed a 4.8 nm DNA tetrahedral nanocage loaded with a hemin-G-quadruplex complex.¹¹⁶ In healthy mice, it was rapidly cleared via glomerular filtration within 2 h. However, in acute kidney injury (AKI) models, the same nanocage showed prolonged retention (≥ 4 h) specifically in renal tubules, demonstrating disease-selective accumulation. This work highlights how ultrasmall, structurally defined DNA carriers can exploit pathological changes in kidney permeability to achieve targeted delivery, providing a novel carrier platform.

Targeting and Functional Moieties

A targeted delivery system relies not only on the carrier itself but also heavily on various modifications applied to the carrier. Some of these modifications can enhance the overall stability of the system and significantly improve its renal targeting efficiency. Furthermore, for systems designed to enable condition-responsive drug release, the design and composition of such modifications are critically important (Table 5).

Molecular Recognition (Ligands)

Peptides & Aptamers

Peptide-based ligands are one of the most widely studied targeting moieties, owing to their design flexibility, moderate immunogenicity, and ability to mimic natural protein-protein interactions. The kidney-targeting peptide (KTP), which binds to megalin and cubilin on proximal tubular epithelial cells, is a prominent example and has been successfully integrated into various delivery platforms, demonstrating enhanced renal accumulation across multiple studies.^{47,48,50,73,85,89,95,119–121,123} Beyond its foundational role, the versatility of peptide-based targeting is further illustrated by its successful application across a spectrum of kidney diseases. Figure 4 synthesizes ex vivo imaging and quantitative data from multiple studies, indicating the significant renal accumulation achieved by peptide-functionalized carriers in diverse pathological contexts. While KTP serves as a prominent exemplar in this category, it is important to note that a growing repertoire of disease-specific peptides has been developed to address distinct renal pathophysiology. This collective evidence underscores peptides as a highly adaptable and effective class of targeting ligands, capable of being tailored to various renal cell types and disease states. These include the RIP1 peptide targeting TGF- β 1,¹²⁸ the ZPDGF β R affibody for platelet-derived growth factor β receptor,¹²⁸ a CD70-targeting peptide for renal cell carcinoma,³³ the fibronectin-binding pentapeptide CREKA,¹⁰³ the VCAM-1-binding

Table 5 Molecular Recognition (Ligands)

Type	Name	Target	PMID
Peptide	KTP	Megalín/Cubilín	27784692; 32464235; 38688026; 37121517; 33005739; 38652072; 33130676; 31635263; 31534545; 41390419; [ref: ^{47,48,50,73,85,89,95,119-121}]
	RIPΔ	TGF-β1	38880023[ref: ¹²⁸]
	ZPDGFβR	Platelet-derived growth factor β receptor (PDGFβR)	38880023[ref: ¹²⁸]
	CD70-targeting peptide	CD70	36500549[ref: ³³]
	Pentapeptide CREKA	Fibronectin	31931051[ref: ¹²⁹]
	VHPKQHRGGSKGC	VCAM-1	34925707[ref: ¹³⁰]
	ET peptide	LRG1	39185720[ref: ¹³¹]
	LTH	Megalín	36719986[ref: ²⁶]
	RGD	Fibronectin	38652072[ref: ⁸⁹]
	RWRNM peptide	αvβ3 integrin	34352625[ref: ¹²]
Aptamer	RLS-2	EPB41L5	40178289[ref: ¹³²]
Antibody	Anti-GPR97	GPR97	35643195[ref: ¹²³]
	cG250-TNF	CAIX	19384924[ref: ¹⁰²]
	PSGL-1	P-selectin	38631490[ref: ¹²²]
	Anti-α8 integrin	α8 integrin	34968038[ref: ¹³³]
Natural Ligands	L-serine	Alanine-Serine-Cysteine Transporter 2 (ASCT2)	36145694; 41481962[ref: ^{53,134}]
	2-glucosamine	Megalín	32322470[ref: ¹³⁵]
	BSA	Megalín	35835398[ref: ¹³⁶]
	HSA	Megalín	35803437[ref: ⁸⁷]
	Fuoidan	P-selectin	33253922[ref: ⁹³]
	Glucose	GLUT1	32937179[ref: ¹³⁷]
	HA	CD44	36442556; 36440107[ref: ^{102,133}]
	Folic acid	FRα	33801911; 35872158[ref: ^{91,130}]
	Integrin α ₄ β ₁ , α ₅ β ₁ , α _L β ₂ , and α _M β ₂	VCAM-1/ICAM-1	32851154[ref: ²¹]
Small molecules	Polymeric plerixafor	CXCR4	35394757[ref: ⁸³]
	α-cyclam- <i>p</i> -toluic acid	CXCR4	35552115[ref: ⁷⁶]
	Acetazolamide derivative	CAIX	26912427[ref: ³⁴]

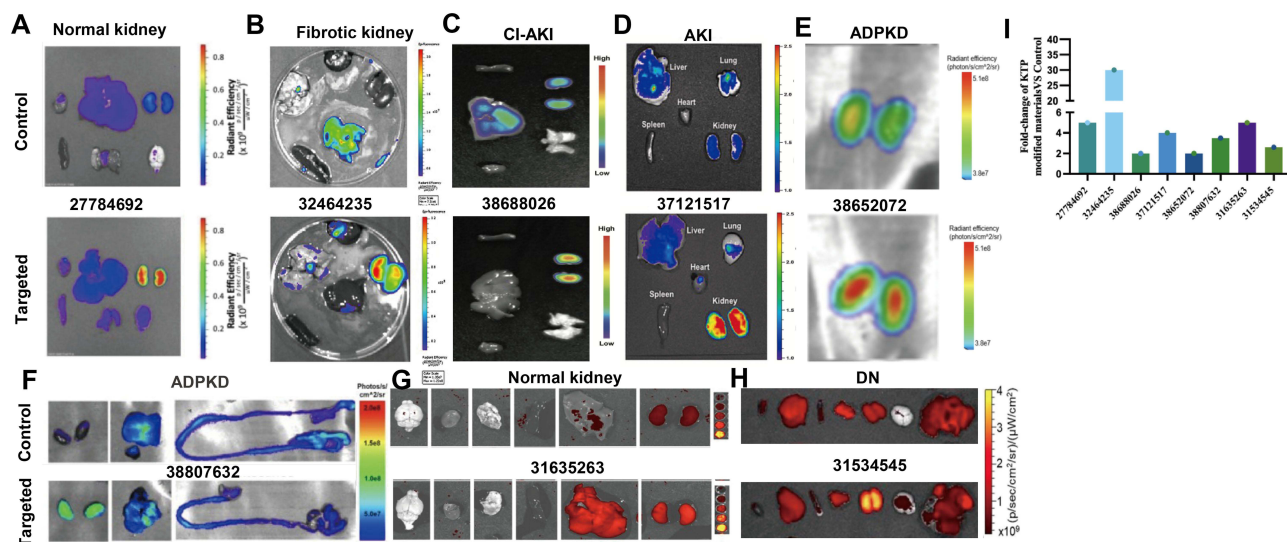


Figure 4 Representative examples of peptide-based renal targeting across kidney diseases. **(A–H)** Ex vivo imaging analysis of renal targeting efficacy. **(I)** Fluorescence-based analysis of renal targeting efficiency of KTPs across different kidney conditions. This figure includes cropped selections from published images obtained copyright permission. The numbers presented in figures are PMID of these studies.

peptide VHPKQHRGGSKGC,³¹ the LRG1-specific ET peptide,¹³¹ the megalin-binding LTH peptide,²⁶ the RGD peptide for integrin $\alpha\beta3$,⁸⁹ and the RWrNM peptide also targeting $\alpha\beta3$ integrin.¹² While peptides offer modular design and good biocompatibility, their susceptibility to proteolytic degradation and modest binding affinity in some cases has spurred the development of alternative ligand classes. Among these, aptamers represent a promising nucleic acid-based targeting strategy, characterized by high specificity, tunable affinity, and enhanced stability against enzymatic degradation. One notable example is RLS-2, which targets EPB41L5 of injured podocytes in Glomerular Diseases, it's remarkable that Both RLS-2 and the scrambled control aptamer exhibited primary accumulation in the kidneys, this biodistribution profile aligns with the known pharmacokinetics of small nucleic acids and confirms the efficient renal delivery of the aptamer platform, which is a prerequisite for targeted podocyte therapy.¹³²

Antibodies & Antibody Fragments

For applications requiring high affinity and established clinical relevance, antibodies serve as powerful targeting tools. They provide precise recognition of overexpressed renal antigens, such as in the case of an anti-GPR97 antibody for injured tubular cells,¹²³ the cG250-TNF antibody targeting CAIX in renal cell carcinoma,¹⁰² PSGL-1 for P-selectin on inflamed endothelium,¹²² and an anti- $\alpha8$ integrin antibody for fibrotic kidneys.¹³⁸

Natural Ligands & Small Molecules

Beyond antibodies, natural ligands offer a distinct advantage by leveraging intrinsic biological recognition pathways, which often result in lower immunogenicity and enhanced biocompatibility. In addition to synthetic ligands, natural ligands are frequently employed to exploit inherent biorecognition pathways within the kidney. This category includes L-serine, which targets the ASCT2 transporter,^{53,97} 2-glucosamine, BSA, and HSA, all targeting megalin,^{87,135,136} fucoidan for P-selectin,⁹³ glucose for glucose transporter 1 (GLUT1) in diabetic nephropathy,¹³⁷ hyaluronic acid (HA) for CD44 on injured cells,^{101,133} folic acid for FR α ,^{91,130} and various integrin ligands ($\alpha4\beta1$, $\alpha5\beta1$, $\alphaL\beta2$, $\alphaM\beta2$) that bind to VCAM-1/ICAM-1.²¹

Complementing these biological and macromolecular approaches, small molecule ligands provide unique benefits such as ease of synthesis, structural versatility, and the potential for oral bioavailability. Finally, small molecule ligands represent another important class, particularly for targeting specific receptors implicated in kidney pathology. Examples

include polymeric plerixafor⁸³ and α -cyclam-p-toluic acid,⁷⁶ both of which target the CXCR4 receptor, as well as acetazolamide derivatives designed for CAIX in renal cell carcinoma.³⁴

The comparative efficacy of these diverse ligand classes-spanning peptides, antibodies, natural ligands, and small molecules were presented in Figure 5, which summarizes their renal targeting performance in different kidney diseases.

Stimuli-Responsive Elements

Stimuli-responsive elements enable spatiotemporally controlled drug release within the pathological renal microenvironment, thereby enhancing therapeutic precision and minimizing systemic side effects. These systems are designed to respond to disease-specific cues, such as elevated reactive oxygen species (ROS), acidic pH, or overexpressed enzymes. For instance, ROS-responsive HATM@RAP nanoparticles can selectively release rapamycin in high-ROS injury sites through CD44-mediated anchoring,¹³³ while the pH-sensitive Lu-CA-CS platform uses megalin receptor-mediated uptake and acidic microenvironment-triggered drug release.⁸⁷ Additionally, enzyme-responsive systems utilize upregulated enzymes such as GGT in diabetic nephropathy for targeted drug activation.^{63,85} External triggers, including ultrasound and magnetic fields, have also been integrated into delivery platforms to enable non-invasive, on-demand release.^{70,97} These intelligent response mechanisms ensure that therapeutic agents are predominantly released at the disease site, thereby improving efficacy and safety.

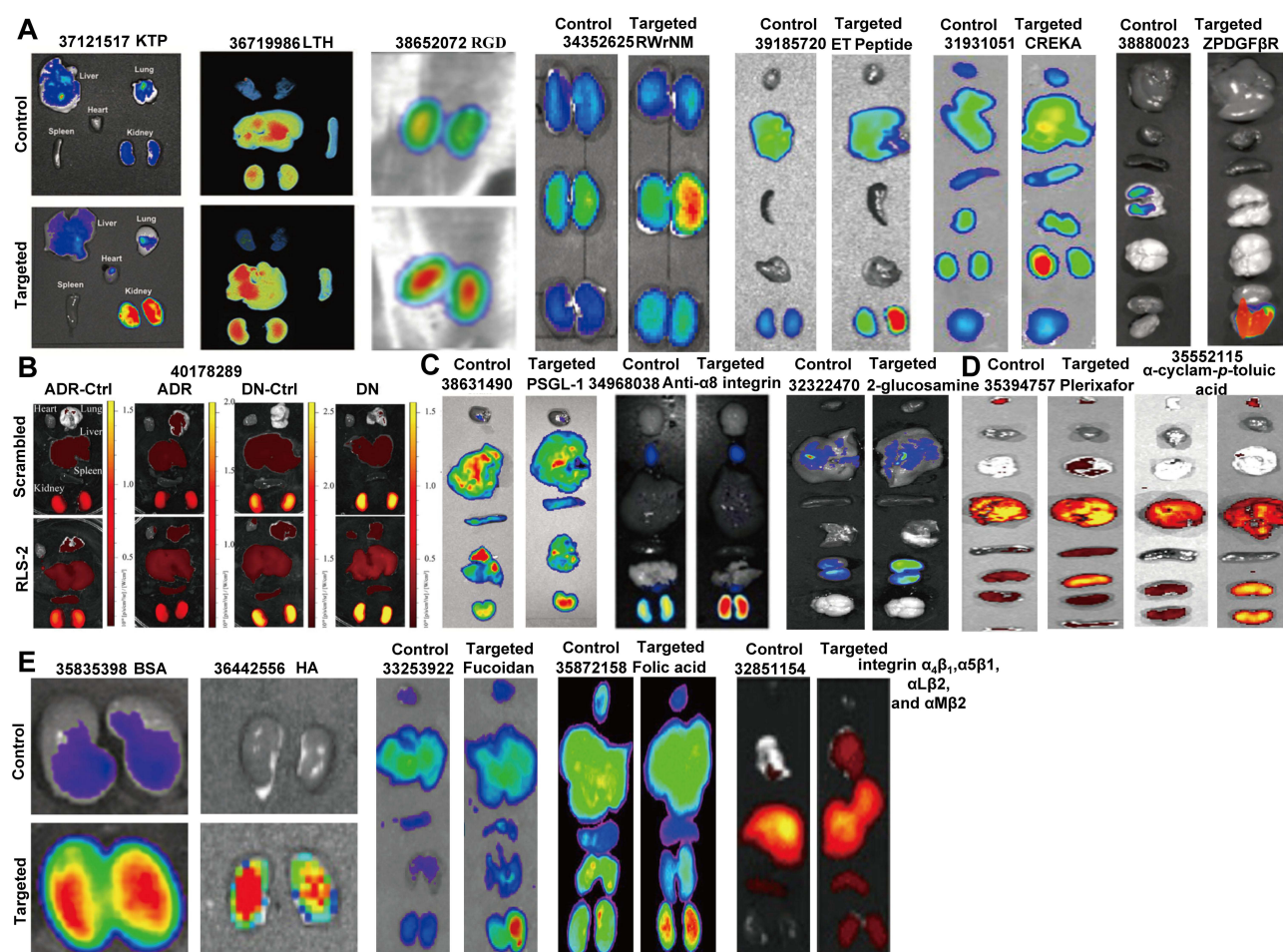


Figure 5 Ex vivo imaging of different targeting ligands in diverse kidney condition. (A) Peptides. (B) Targeted aptamers can not only actively bind to specific cells, but also inherently accumulate in the kidneys due to their small molecular size. (C) Antibodies & antibody fragments. (D) Small molecules. (E) Natural ligands. This figure includes cropped selections from published images obtained copyright permission. The numbers presented in figures are PMID of these studies.

Stealth& Stability Modifications

Surface modifications are essential to enhance the pharmacokinetic profile and biocompatibility of kidney-targeted delivery systems. Polyethylene glycol (PEG) coating is a widely adopted strategy to improve hydrophilicity, reduce opsonization, and prolong circulation half-life, as demonstrated in PEGylated PLGA and lipid-based systems.^{36,98} Beyond PEGylation, biomimetic coatings, such as platelet or renal tubular epithelial cell membranes also provide natural “self-recognition” properties that further enhance targeting and reduce immune clearance.^{32,114} Charge modulation, particularly the use of cationic polymers like chitosan, can enhance renal retention through electrostatic interactions with negatively charged glomerular structures, though careful design is required to mitigate potential cytotoxicity.¹²⁹ Additionally, polysaccharide-based coatings such as hyaluronic acid and chitosan can also contribute to stability and renal affinity while supporting ligand presentation.^{101,133} Together, these modifications collectively enhance systemic stability, prolong circulation, and facilitate efficient renal accumulation.

Therapeutic Cargo Considerations

While the primary focus of this review is the targeting system, the therapeutic cargo, encompassing small molecules, nucleic acids, proteins, peptides, and imaging agents fundamentally determines the pharmacological outcome. Effective delivery requires careful matching of cargo properties with carrier design. Hydrophobic small molecules are often encapsulated within lipid cores or polymeric matrices, while hydrophilic or charged macromolecules may be electrostatically complexed or covalently conjugated.

A critical advancement is the rational co-design of cargo and delivery system, where the carrier or ligand itself contributes therapeutic activity. For instance, bilirubin-loaded or melanin-based nanoparticles function dually as anti-oxidative agents and drug carriers.^{77,123} Similarly, siRNA designed to silence fibrosis-related genes can be co-delivered with anti-fibrotic peptides, creating a synergistic “drug & carrier” therapeutic package.²¹ In other systems, the targeting ligand may also serve as the primary therapeutic, with the nanoparticle primarily functioning as a stabilizer and targeting enhancer.^{34,76,83}

Thus, the integration of cargo characteristics with the physicochemical and targeting properties of the delivery platform is essential for developing next-generation, high-efficacy renal nanotherapeutics.

Discussion

Biological Barriers and Strategies

Fenestrated glomerular endothelium, charged basement membrane, and the intricate slit of podocytes consist the multi-layered filtration system, thus acts as a precise molecular sieve. Upon entering the renal circulation, systemically administered nanocarriers face a tripartite fate that dictates their therapeutic potential, firstly, nonspecific clearance via the reticuloendothelial system (primarily liver and spleen); Secondly, passaging through the glomerulus followed by potential urinary excretion, or thirdly, active engagement with renal cells via transcytosis, retention, or receptor-mediated uptake. Strategic engineering of nanocarriers is aimed at navigating this fate map. To avoid off-target sequestration, stealth modifications like PEGylation or the use of zwitterionic coatings are employed to minimize clearance and prolong circulation. To harness the kidney’s inherent filtration for delivery, particles can be engineered within a strict size window (typically <6–8 nm) and often benefit from a neutral or slightly positive surface charge to counteract the negative charge of the glomerular basement membrane. For those carriers designed to target specific renal compartments instead of rapid excretion, larger sizes and active targeting ligands become essential. These ligands serve as molecular addresses to convert nonspecific distribution into precise homing. Thus, the first principle of renal nanomedicine is a barrier-centric design, where physicochemical properties are meticulously modulated to cooperate with, rather than fight against renal physiology.

The Emergency of Integrated and Synergistic Design

The field of kidney-targeted drug delivery has matured significantly, yielding a substantial body of literature that expertly categorizes strategies by nanoparticle material, physicochemical property, or target renal cell type.^{5,139–141} However, as

the complexity of nanocarrier design advances—incorporating active targeting, stimuli-responsive release, and multi-modal functionalities, a mere cataloging of components becomes insufficient to guide the next generation of therapeutics.

Our review proposes an integrative, engineering-oriented design framework. Rather than following a conventional structure organized by material or anatomy, we deconstruct kidney-targeted systems into interoperable modules: Carrier Platforms, Targeting & Functional Moieties, Stimuli-Responsive Elements, and Therapeutic Cargo. This modular perspective allows for a critical analysis not just of individual components, but of their synergistic combinations.

The H-Dot nanoparticle, for instance, is engineered with an ultrafilterable size (<10 nm) to passively reach the urinary space, where it then leverages a cilastatin ligand for active uptake by megalin-expressing proximal tubules, resulting in remarkable renal specificity and minimal systemic exposure.¹⁴² Another example is the convergence of targeting with microenvironmental intelligence. The HATM@RAP system employs hyaluronic acid to anchor to CD44-overexpressing injured cells, while a built-in ROS-responsive linker ensures drug release is contingent upon the pathological oxidative stress within the target niche.¹³³ Further combination is seen in multi-component systems like the orally administered, yeast-cell-wall-based “hitchhiking” platform, which integrates drug delivery with probiotic-mediated gut-renal axis modulation.¹⁴³ These examples indicate a pivotal shift: the frontier is no longer dominated by novel materials alone, but by novel integrations that create logically orchestrated, multi-stage delivery cascades.

Future Prospects and Challenges

The quest for optimal nanocarriers is evolving from casual discovery to rational, data-driven design. Smith et al employed a high-throughput DNA-barcoded screening platform to systematically evaluate the *in vivo* organ targeting of hundreds of nanoparticles with diverse physicochemical properties.¹³⁴ This “big data” approach led to the identification of a lead candidate, the “M5N” nanocarrier, which demonstrated exceptional specificity for kidney delivery, particularly to tubular epithelial cells. Its renal targeting was found to be a sequential process involving initial passive glomerular filtration due to its size, followed by active uptake via the megalin receptor on proximal tubules, this is a classic “passive + active” synergy uncovered by systematic screening. This study provides a powerful blueprint for the future, leveraging combinatorial libraries and high-throughput *in vivo* screening to rapidly identify optimal carrier platforms, thereby accelerating the development of targeted delivery systems for the kidney and beyond.

Despite these exciting advances, persistent challenges must be addressed. Evading liver uptake and ensuring safe clearance constitute central challenges in kidney-targeted drug delivery. The majority of systemically administered nanoparticles are intercepted by the liver, significantly diminishing the bioavailable dose for renal action. Current strategies extend beyond conventional PEGylation and include emerging approaches such as zwitterionic coatings to reduce protein adsorption and biomimetic camouflage using cell membranes. For instance, the Selective Organ Targeting (SORT) platform enables lipid nanoparticles to preferentially accumulate in the kidneys rather than the liver through rational lipid composition design alone.¹⁰⁰ On the other hand, the safe clearance of carriers is equally critical. Designing nanoparticles that are either small enough for renal filtration or fully biodegradable represents a viable pathway, as exemplified by certain carbon dots or degradable silica-based systems.^{112,113} The ideal future system must therefore achieve a precise balance between “escaping the liver” and “being recognized or cleared by the kidney,” which remains a pivotal design hurdle for future translation. In addition, batch-to-batch variability in complex formulations, especially for bio-derived carriers like exosomes, demands rigorous manufacturing standards. Perhaps most critically, the heterogeneity of human kidney diseases means that a “one size fits all” nanocarrier is unlikely. Future delivery may depend on patient stratification and the development of modular platforms adaptable to different pathological signatures.⁹⁵

Conclusions

In conclusion, successful kidney-targeted drug delivery requires moving beyond isolated strategies. Effective systems must be an integrated design: combine the renal enrichment offered by passive targeting with the cellular specificity conferred by active targeting ligands. This core combination is further enhanced by incorporating stimuli-responsive elements that control drug release within disease-specific microenvironments. Despite remaining challenges, this integrated approach represents the most promising path forward. The continued development of such multifunctional platforms is essential for achieving precise and effective therapies for kidney diseases.

Abbreviations

AKI, acute kidney injury; CKD, chronic kidney disease; GFB, glomerular filtration barrier; GBM, glomerular basement membrane; ECs, endothelial cells; PTECs, proximal tubular epithelial cells; RBF, renal blood flow; DN, diabetic nephropathy; OAT1–4, organic anion transporters; ROS, reactive oxygen species; RCC, renal cell carcinoma; GGT, γ -glutamyl transpeptidase; EV, extracellular vesicle; NPs, Polymeric Nanoparticles; PLGA, poly(lactic-co-glycolic acid); IR, ischemic-reperfusion; CZ-PLGA-NPs, cabozantinib-loaded PLGA NPs; PEG, polyethylene glycol; KTP, kidney-targeting peptide; HAS, human serum albumin; PEI, polyethylenimine; PPS-PEI, polypropylene sulfide-polyethylenimine; PPs, plerixafor-based polycations; PGA, poly- γ -glutamic acid; LNPs, Lipid Nanoparticles; SORT, Selective Organ Targeting; PA, phosphatidic acid; HDL, High-density lipoprotein; MSCs, mesenchymal stem cells; AuNPs, Gold nanoparticles; Zt-SeCDs, Selenium-doped carbon dots; mSiO₂, mesoporous silica; SCLMs, silica-cross-linked micelles; MOFs, Metal–Organic Framework; Ga NDs, Gallium nanodroplets; ZIF-8, zeolite imidazolate framework-8; ELPs, Elastin-like Polypeptides; cBSA, Cationic bovine serum albumin; LMWPs, Low Molecular Weight Proteins; UTMD, ultrasound-targeted microbubble destruction; PMVs, Platelet membrane vesicles; PSGL-1, P-selectin glycoprotein ligand-1; UCNPs, upconversion nanoparticles; MNPs, Melanin Nanoparticles; PA, photoacoustic; IN, Inulin; GLUT1, glucose transporter 1; HA, hyaluronic acid; PEG, Polyethylene glycol.

Author Contributions

All authors made a significant contribution to the work reported, whether that is in the conception, study design, execution, acquisition of data, analysis and interpretation, or in all these areas; took part in drafting, revising or critically reviewing the article; gave final approval of the version to be published; have agreed on the journal to which the article has been submitted; and agree to be accountable for all aspects of the work.

Funding

There is no funding to report.

Disclosure

The authors declare that they have no competing interests.

References

- Osborn JW, Tyshynsky R, Vulchanova L. Function of renal nerves in kidney physiology and pathophysiology. *Ann Rev Physiol.* 2021;83(1):429–450. doi:10.1146/annurev-physiol-031620-091656
- Câmara NO, Iseki K, Kramer H, Liu ZH, Sharma K. Kidney disease and obesity: epidemiology, mechanisms and treatment. *Nat Rev Nephrol.* 2017;13(3):181–190. doi:10.1038/nrneph.2016.191
- Dubin RF, Rhee EP. Proteomics and metabolomics in kidney disease, including insights into etiology, treatment, and prevention. *Clin J Am Soc Nephrol.* 2020;15(3):404–411. doi:10.2215/cjn.07420619
- Lu J, Xu X, Sun X, Du Y. Protein and peptide-based renal targeted drug delivery systems. *J Control Release.* 2024;366:65–84. doi:10.1016/j.jconrel.2023.12.036
- Huang Y, Wang J, Jiang K, Chung EJ. Improving kidney targeting: the influence of nanoparticle physicochemical properties on kidney interactions. *J Control Release.* 2021;334:127–137. doi:10.1016/j.jconrel.2021.04.016
- Di L. An update on the importance of plasma protein binding in drug discovery and development. *Expert Opin Drug Discov.* 2021;16(12):1453–1465. doi:10.1080/17460441.2021.1961741
- Huang X, Ma Y, Li Y, Han F, Lin W. Targeted drug delivery systems for kidney diseases. *Front Bioeng Biotechnol.* 2021;9:683247. doi:10.3389/fbioe.2021.683247
- Khare V, Cherqui S. Targeted gene therapy for rare genetic kidney diseases. *Kidney Int.* 2024;106(6):1051–1061. doi:10.1016/j.kint.2024.07.034
- Huang S, Ren Y, Wang X, et al. Application of ultrasound-targeted microbubble destruction-mediated exogenous gene transfer in treating various renal diseases. *Hum Gene Ther.* 2019;30(2):127–138. doi:10.1089/hum.2018.070
- Grahammer F, Schell C, Huber TB. The podocyte slit diaphragm—from a thin grey line to a complex signalling hub. *Nat Rev Nephrol.* 2013;9(10):587–598. doi:10.1038/nrneph.2013.169
- Bruni R, Possenti P, Bordignon C, et al. Ultrasmall polymeric nanocarriers for drug delivery to podocytes in kidney glomerulus. *J Control Release.* 2017;255:94–107. doi:10.1016/j.jconrel.2017.04.005
- Huang C, Zhao X, Su M, Yin Z. Construction and evaluation of novel $\alpha\beta 3$ integrin ligand-conjugated ultrasmall star polymer micelles targeted glomerular podocytes through GFB permeation. *Biomaterials.* 2021;276:121053. doi:10.1016/j.biomaterials.2021.121053
- Hu S, Hang X, Wei Y, Wang H, Zhang L, Zhao L. Crosstalk among podocytes, glomerular endothelial cells and mesangial cells in diabetic kidney disease: an updated review. *Cell Commun Signaling.* 2024;22(1):136. doi:10.1186/s12964-024-01502-3

14. Zhang D, Wei C, Hop C, et al. Intestinal excretion, intestinal recirculation, and renal tubule reabsorption are underappreciated mechanisms that drive the distribution and pharmacokinetic behavior of small molecule drugs. *J Med Chem.* 2021;64(11):7045–7059. doi:10.1021/acs.jmedchem.0c01720
15. Huang Y, Ning X, Ahrari S, et al. Physiological principles underlying the kidney targeting of renal nanomedicines. *Nat Rev Nephrol.* 2024;20(6):354–370. doi:10.1038/s41581-024-00819-z
16. Wang J, Masehi-Lano JJ, Chung EJ. Peptide and antibody ligands for renal targeting: nanomedicine strategies for kidney disease. *Biomater Sci.* 2017;5(8):1450–1459. doi:10.1039/c7bm00271h
17. Wu L, Chen M, Mao H, et al. Albumin-based nanoparticles as methylprednisolone carriers for targeted delivery towards the neonatal Fc receptor in glomerular podocytes. *Int J Mol Med.* 2017;39(4):851–860. doi:10.3892/ijmm.2017.2902
18. Tripathy N, Wang J, Tung M, Conway C, Chung EJ. Transdermal delivery of kidney-targeting nanoparticles using dissolvable microneedles. *Cell Mol Bioeng.* 2020;13(5):475–486. doi:10.1007/s12195-020-00622-3
19. Seron D, Cameron JS, Haskard DO. Expression of VCAM-1 in the normal and diseased kidney. *Nephrol Dial Transplant.* 1991;6(12):917–922. doi:10.1093/ndt/6.12.917
20. Singh V, Kaur R, Kumari P, Pasricha C, Singh R. ICAM-1 and VCAM-1: gatekeepers in various inflammatory and cardiovascular disorders. *Clin Chim Acta.* 2023;548:117487. doi:10.1016/j.cca.2023.117487
21. Tang TT, Wang B, Wu M, et al. Extracellular vesicle-encapsulated IL-10 as novel nanotherapeutics against ischemic AKI. *Sci Adv.* 2020;6(33):eaaz0748. doi:10.1126/sciadv.aaz0748
22. Pollinger K, Hennig R, Breunig M, et al. Kidney podocytes as specific targets for cyclo(RGDfC)-modified nanoparticles. *Small.* 2012;8(21):3368–3375. doi:10.1002/sml.201200733
23. Liu H, Zhang H, Yin N, et al. Sialic acid-modified dexamethasone lipid calcium phosphate gel core nanoparticles for target treatment of kidney injury. *Biomater Sci.* 2020;8(14):3871–3884. doi:10.1039/d0bm00581a
24. McEver RP, Cummings RD. Perspectives series: cell adhesion in vascular biology. Role of PSGL-1 binding to selectins in leukocyte recruitment. *J Clin Invest.* 1997;100(3):485–491. doi:10.1172/jci119556
25. Huang C, Zeng T, Li J, et al. Folate receptor-mediated renal-targeting nanopatform for the specific delivery of triptolide to treat renal ischemia/reperfusion injury. *ACS Biomater Sci Eng.* 2019;5(6):2877–2886. doi:10.1021/acsbomaterials.9b00119
26. Yan J, Wang Y, Zhang J, Liu X, Yu L, He Z. Rapidly blocking the calcium overload/ROS production feedback loop to alleviate acute kidney injury via microenvironment-responsive BAPTA-AM/BAC co-delivery nanosystem. *Small.* 2023;19(17):e2206936. doi:10.1002/sml.202206936
27. Sutton TA. Alteration of microvascular permeability in acute kidney injury. *Microvascular Res.* 2009;77(1):4–7. doi:10.1016/j.mvr.2008.09.004
28. Hryciw DH, Lee EM, Pollock CA, Poronnik P. Molecular changes in proximal tubule function in diabetes mellitus. *Clin Experiment Pharmacol Physiol.* 2004;31(5–6):372–379. doi:10.1111/j.1440-1681.2004.04001.x
29. Sun H, Frassetto L, Benet LZ. Effects of renal failure on drug transport and metabolism. *Pharmacol Ther.* 2006;109(1–2):1–11. doi:10.1016/j.pharmthera.2005.05.010
30. Guo H, Lan T, Lu X, et al. ROS-responsive curcumin-encapsulated nanoparticles for AKI therapy via promoting lipid degradation in renal tubules. *J Mat Chem B.* 2024;12(12):3063–3078. doi:10.1039/d3tb02318d
31. Wu Q, Wang J, Wang Y, et al. Targeted delivery of celastrol to glomerular endothelium and podocytes for chronic kidney disease treatment. *Nano Res.* 2022;15(4):3556–3568. doi:10.1007/s12274-021-3894-x
32. Fei S, Ma Y, Zhou B, et al. Platelet membrane biomimetic nanoparticle-targeted delivery of TGF- β 1 siRNA attenuates renal inflammation and fibrosis. *Int J Pharm.* 2024;659:124261. doi:10.1016/j.ijpharm.2024.124261
33. Trac N, Oh HS, Jones LI, et al. CD70-targeted micelles enhance HIF2 α siRNA delivery and inhibit oncogenic functions in patient-derived clear cell renal carcinoma cells. *Molecules.* 2022;27(23):8457. doi:10.3390/molecules27238457
34. Krall N, Pretto F, Mattarella M, Müller C, Neri D. A 99mTc-labeled ligand of carbonic anhydrase IX selectively targets renal cell carcinoma in vivo. *J Nucl Med.* 2016;57(6):943–949. doi:10.2967/jnumed.115.170514
35. Cazzamalli S, Dal Corso A, Neri D. Acetazolamide serves as selective delivery vehicle for dipeptide-linked drugs to renal cell carcinoma. *Mol Cancer Ther.* 2016;15(12):2926–2935. doi:10.1158/1535-7163.Mct-16-0283
36. Yamaguchi S, Sedaka R, Kapadia C, et al. Rapamycin-encapsulated nanoparticle delivery in polycystic kidney disease mice. *Sci Rep.* 2024;14(1):15140. doi:10.1038/s41598-024-65830-7
37. Du B, Jiang X, Das A, et al. Glomerular barrier behaves as an atomically precise bandpass filter in a sub-nanometre regime. *Nature Nanotechnol.* 2017;12(11):1096–1102. doi:10.1038/nnano.2017.170
38. Li Y, Wang G, Wang T, et al. PEGylated gambogic acid nanoparticles enable efficient renal-targeted treatment of acute kidney injury. *Nano Lett.* 2023;23(12):5641–5647. doi:10.1021/acs.nanolett.3c01235
39. Williams RM, Shah J, Ng BD, et al. Mesoscale nanoparticles selectively target the renal proximal tubule epithelium. *Nano Lett.* 2015;15(4):2358–2364. doi:10.1021/nl504610d
40. Prikhozhenko ES, Gusliakova OI, Kulikov OA, et al. Target delivery of drug carriers in mice kidney glomeruli via renal artery. Balance between efficiency and safety. *J Control Release.* 2021;329:175–190. doi:10.1016/j.jconrel.2020.11.051
41. Sancey L, Kotb S, Truillet C, et al. Long-term in vivo clearance of gadolinium-based AGuIX nanoparticles and their biocompatibility after systemic injection. *ACS nano.* 2015;9(3):2477–2488. doi:10.1021/acsnano.5b00552
42. Liu D, Shu G, Jin F, et al. ROS-responsive chitosan-SS31 prodrug for AKI therapy via rapid distribution in the kidney and long-term retention in the renal tubule. *Sci Adv.* 2020;6(41). doi:10.1126/sciadv.abb7422
43. Xie D, Wang J, Hu G, et al. Kidney-targeted delivery of prolyl hydroxylase domain protein 2 small interfering rna with nanoparticles alleviated renal ischemia/reperfusion injury. *J Pharmacol Exp Ther.* 2021;378(3):235–243. doi:10.1124/jpet.121.000667
44. Kok RJ, Haas M, Mooleenaar F, de Zeeuw D, Meijer DK. Drug delivery to the kidneys and the bladder with the low molecular weight protein lysozyme. *Renal failure.* 1998;20(2):211–217. doi:10.3109/08860229809045104
45. Chen D, Xu J, Lv S, et al. Enzyme-activatable kidney-targeted dendrimer-drug conjugate for efficient childhood nephrotic syndrome therapy. *Theranostics.* 2024;14(18):6991–7006. doi:10.7150/thno.101606

46. Geng Q, Sun X, Gong T, Zhang ZR. Peptide-drug conjugate linked via a disulfide bond for kidney targeted drug delivery. *Bioconjugate Chem.* 2012;23(6):1200–1210. doi:10.1021/bc300020f
47. He J, Chen H, Zhou W, et al. Kidney targeted delivery of asiatic acid using a FITC labeled renal tubular-targeting peptide modified PLGA-PEG system. *Int J Pharm.* 2020;584:119455. doi:10.1016/j.ijpharm.2020.119455
48. Huang Z, Chun C, Li X. Kidney targeting peptide-modified biomimetic nanoplatforams for treatment of acute kidney injury. *J Control Release.* 2023;358:368–381. doi:10.1016/j.jconrel.2023.04.042
49. He H, Halseth TA, Mei L, Shen C, Liu L, Schwendeman A. Nanodisc delivery of liver X receptor agonist for the treatment of diabetic nephropathy. *J Control Release.* 2022;348:1016–1027. doi:10.1016/j.jconrel.2022.06.029
50. Huang Y, Jiang K, Zhang X, Chung EJ. The effect of size, charge, and peptide ligand length on kidney targeting by small, organic nanoparticles. *Bioeng Transl Med.* 2020;5(3):e10173. doi:10.1002/btm2.10173
51. Lewington AJ, Padanilam BJ, Martin DR, Hammerman MR. Expression of CD44 in kidney after acute ischemic injury in rats. *Am J Physiol Regulat.* 2000;278(1):R247–54. doi:10.1152/ajpregu.2000.278.1.R247
52. Huang ZW, Shi Y, Zhai YY, et al. Hyaluronic acid coated bilirubin nanoparticles attenuate ischemia reperfusion-induced acute kidney injury. *J Control Release.* 2021;334:275–289. doi:10.1016/j.jconrel.2021.04.033
53. Katsumi H, Kitada S, Yasuoka S, et al. L-Serine-modified poly-L-lysine as a biodegradable kidney-targeted drug carrier for the efficient radionuclide therapy of renal cell carcinoma. *Pharmaceutics.* 2022;14(9):1946. doi:10.3390/pharmaceutics14091946
54. Chen W, Zhang A, Li S-D. Limitations and niches of the active targeting approach for nanoparticle drug delivery. *Eur J Nanomed.* 2012;4(2–4):89–93. doi:10.1515/ejnm-2012-0010
55. Cheng WW, Allen TM. Targeted delivery of anti-CD19 liposomal doxorubicin in B-cell lymphoma: a comparison of whole monoclonal antibody, Fab' fragments and single chain Fv. (1873-4995 (Electronic)). *J Contr Release.* 2008;126(1):50–58.
56. Collins D, Huang L. Cytotoxicity of diphtheria toxin A fragment to toxin-resistant murine cells delivered by pH-sensitive immunoliposomes. (0008-5472 (Print)). *Cancer Res.* 1987;47(3):735–739.
57. Rahme K, Dagher N. Chemistry routes for copolymer synthesis containing peg for targeting, imaging, and drug delivery purposes. *Pharmaceutics.* 2019;11(7):327. doi:10.3390/pharmaceutics11070327
58. Williams RM, Shah J, Mercer E, et al. Kidney-targeted redox scavenger therapy prevents cisplatin-induced acute kidney injury. *Front Pharmacol.* 2021;12:790913. doi:10.3389/fphar.2021.790913
59. Guo X, Xu L, Velazquez H, et al. Kidney-targeted renalase agonist prevents cisplatin-induced chronic kidney disease by inhibiting regulated necrosis and inflammation. *J Am Soc Nephrol.* 2022;33(2):342–356. doi:10.1681/asn.2021040439
60. Han SJ, Williams RM, D'Agati V, Jaimes EA, Heller DA, Lee HT. Selective nanoparticle-mediated targeting of renal tubular Toll-like receptor 9 attenuates ischemic acute kidney injury. *Kidney Int.* 2020;98(1):76–87. doi:10.1016/j.kint.2020.01.036
61. Lai X, Geng X, Tan L, Hu J, Wang S. A pH-responsive system based on fluorescence enhanced gold nanoparticles for renal targeting drug delivery and fibrosis therapy. *Int J Nanomed.* 2020;15:5613–5627. doi:10.2147/ijn.S260069
62. Oroojalian F, Rezayan AH, Mehrnejad F, et al. Efficient megalin targeted delivery to renal proximal tubular cells mediated by modified-polymyxin B-polyethylenimine based nano-gene-carriers. *Mater Sci Eng C.* 2017;79:770–782. doi:10.1016/j.msec.2017.05.068
63. Wang Q, Han S, Zhu Y, Wang G, Chen D. Poly- γ -glutamic acid coating polymeric nanoparticles enhance renal drug distribution and cellular uptake for diabetic nephropathy therapy. *J Drug Targeting.* 2023;31(1):89–99. doi:10.1080/1061186x.2022.2106488
64. Najahi-Missauwi W, Arnold RA-O, Cummings BS. Safe Nanoparticles: are We There Yet? LID - 10.3390/ijms22010385 [doi] LID - 385. (1422-0067 (Electronic)). *Int J Mol Sci.* 2020;22(1):385.
65. Cheng HT, Huang HC, Lee TY, et al. Delivery of sorafenib by myofibroblast-targeted nanoparticles for the treatment of renal fibrosis. *J Control Release.* 2022;346:169–179. doi:10.1016/j.jconrel.2022.04.004
66. Lee HW, Seo HS, Yeom SY, et al. Cabozantinib-loaded PLGA nanoparticles: a potential adjuvant strategy for surgically resected high-risk non-metastatic renal cell carcinoma. *Int J Mol Sci.* 2022;23(20). doi:10.3390/ijms232012634
67. Vallorz EL, Janda J, Mansour HM, Schnellmann RG. Kidney targeting of formoterol containing polymeric nanoparticles improves recovery from ischemia reperfusion-induced acute kidney injury in mice. *Kidney Int.* 2022;102(5):1073–1089. doi:10.1016/j.kint.2022.05.032
68. Liu Q, Chen X, Kan M, et al. Gypenoside XLIX loaded nanoparticles targeting therapy for renal fibrosis and its mechanism. *Eur J Pharmacol.* 2021;910:174501. doi:10.1016/j.ejphar.2021.174501
69. Vallorz EL, Blohm-Mangone K, Schnellmann RG, Mansour HM. Formoterol PLGA-PEG nanoparticles induce mitochondrial biogenesis in renal proximal tubules. *AAPS J.* 2021;23(4):88. doi:10.1208/s12248-021-00619-4
70. Wei S, Xu C, Zhang Y, Shi Z, Wu M, Yang B. Ultrasound Assisted a Peroxisome Proliferator-Activated Receptor (PPAR) γ agonist-loaded nanoparticle-microbubble complex to attenuate renal interstitial fibrosis. *Int J Nanomed.* 2020;15:7315–7327. doi:10.2147/ijn.S262052
71. Yu H, Lin T, Chen W, et al. Size and temporal-dependent efficacy of oltipraz-loaded PLGA nanoparticles for treatment of acute kidney injury and fibrosis. *Biomaterials.* 2019;219:119368. doi:10.1016/j.biomaterials.2019.119368
72. Li S, Zeng YC, Peng K, Liu C, Zhang ZR, Zhang L. Design and evaluation of glomerulus mesangium-targeted PEG-PLGA nanoparticles loaded with dexamethasone acetate. *Acta Pharmacol Sin.* 2019;40(1):143–150. doi:10.1038/s41401-018-0052-4
73. Gu XR, Tai YF, Liu Z, et al. Layer-by-layer assembly of renal-targeted polymeric nanoparticles for robust arginase-2 knockdown and contrast-induced acute kidney injury prevention. *Adv Healthcare Mater.* 2024;13(20):e2304675. doi:10.1002/adhm.202304675
74. Nan S, Che Y, Gong T, Zhang Z, Fu Y. Renal-targeted drug delivery by chitosan oligosaccharide micelles with HSA-enriched protein corona for the treatment of ischemia/reperfusion-induced acute kidney injury. *ACS Appl Mater Interfaces.* 2024;16(37):49913–49925. doi:10.1021/acsami.4c09665
75. Prajapati C, Agrawal YO, Agnihotri VV, et al. Development and biological evaluation of protective effect of kidney targeted N-acetylated chitosan nanoparticles containing thymoquinone for the treatment of DNA damage in cyclophosphamide-induced haemorrhagic cystitis. *Int J Biol Macromol.* 2022;214:391–401. doi:10.1016/j.ijbiomac.2022.06.070
76. Tang W, Panja S, Jogdeo CM, et al. Modified chitosan for effective renal delivery of siRNA to treat acute kidney injury. *Biomaterials.* 2022;285:121562. doi:10.1016/j.biomaterials.2022.121562
77. Wang DW, Li SJ, Tan XY, et al. Engineering of stepwise-targeting chitosan oligosaccharide conjugate for the treatment of acute kidney injury. *Carbohydr Polym.* 2021;256:117556. doi:10.1016/j.carbpol.2020.117556

78. Qiao H, Sun M, Su Z, et al. Kidney-specific drug delivery system for renal fibrosis based on coordination-driven assembly of catechol-derived chitosan. *Biomaterials*. 2014;35(25):7157–7171. doi:10.1016/j.biomaterials.2014.04.106
79. Zhang Q, Li Y, Wang S, et al. Chitosan-based oral nanoparticles as an efficient platform for kidney-targeted drug delivery in the treatment of renal fibrosis. *Int J Biol Macromol*. 2024;256(Pt 1):128315. doi:10.1016/j.ijbiomac.2023.128315
80. Singh AK, Salunkhe SA, Chitkara D, Mittal A. Potent anti-inflammatory and anti-apoptotic activities of electrostatically complexed C-peptide nanospheres ameliorate diabetic nephropathy. *Biomater Adv*. 2024;163:213935. doi:10.1016/j.bioadv.2024.213935
81. Guo L, Yan H, Gong Q, et al. Glomerulus-targeted ROS-responsive polymeric nanoparticles for effective membranous nephropathy therapy. *ACS Appl Mater Interfaces*. 2024;16(27):35447–35462. doi:10.1021/acsami.4c04345
82. Wei H, Jiang D, Yu B, et al. Nanostructured polyvinylpyrrolidone-curcumin conjugates allowed for kidney-targeted treatment of cisplatin induced acute kidney injury. *Bioact Mater*. 2023;19:282–291. doi:10.1016/j.bioactmat.2022.04.006
83. Tang W, Panja S, Jogdeo CM, Tang S, Yu A, Oupický D. Study of renal accumulation of targeted polycations in acute kidney injury. *Biomacromolecules*. 2022;23(5):2064–2074. doi:10.1021/acs.biomac.2c00079
84. Mathew AP, Uthaman S, Bae EH, Lee JY, Park IK. Vimentin targeted nano-gene carrier for treatment of renal diseases. *J Korean Med Sci*. 2021;36(49):e3333. doi:10.3346/jkms.2021.36.e3333
85. Wang G, Li Q, Chen D, et al. Kidney-targeted rhin-loaded liponanoparticles for diabetic nephropathy therapy via size control and enhancement of renal cellular uptake. *Theranostics*. 2019;9(21):6191–6208. doi:10.7150/thno.37538
86. Elmotasem H, Salama AAA, Shalaby ES. Hyaluronate functionalized Span-Labrasol nanovesicular transdermal therapeutic system of ferulic acid targeting diabetic nephropathy. *Int J Biol Macromol*. 2024;279(Pt 3):135292. doi:10.1016/j.ijbiomac.2024.135292
87. Pang M, Duan S, Zhao M, et al. Co-delivery of celastrol and lutein with pH sensitive nano micelles for treating acute kidney injury. *Toxicol Appl Pharmacol*. 2022;450:116155. doi:10.1016/j.taap.2022.116155
88. Bishop BY, Sharma SH, Tiwari R, et al. Enabling organ- and injury-specific nanocarrier targeting via surface-functionalized PEG-b-PPS micelles for acute kidney injury. *Nanoscale Horiz*. 2025;10(12):3423–3432. doi:10.1039/d5nh00474h
89. Huang Y, Osouli A, Pham J, et al. Investigation of basolateral targeting micelles for drug delivery applications in polycystic kidney disease. *Biomacromolecules*. 2024;25(5):2749–2761. doi:10.1021/acs.biomac.3c01397
90. Guo C, Cao M, Diao N, et al. Novel pH-responsive E-selectin targeting natural polysaccharides hybrid micelles for diabetic nephropathy. *Nanomedicine*. 2023;52:102696. doi:10.1016/j.nano.2023.102696
91. Du B, Zhao M, Wang Y, et al. Folic acid-targeted pluronic F127 micelles improve oxidative stress and inhibit fibrosis for increasing AKI efficacy. *Eur J Pharmacol*. 2022;930:175131. doi:10.1016/j.ejphar.2022.175131
92. Kim CS, Mathew AP, Vasukutty A, et al. Glycol chitosan-based tacrolimus-loaded nanomicelle therapy ameliorates lupus nephritis. *J Nanobiotechnol*. 2021;19(1):109. doi:10.1186/s12951-021-00857-w
93. Shu G, Lu C, Wang Z, et al. Fucoidan-based micelles as P-selectin targeted carriers for synergistic treatment of acute kidney injury. *Nanomedicine*. 2021;32:102342. doi:10.1016/j.nano.2020.102342
94. Gu M, Lu L, Wei Q, et al. Improved oral bioavailability and anti-chronic renal failure activity of chrysophanol via mixed polymeric micelles. *J Microencaps*. 2021;38(1):47–60. doi:10.1080/02652048.2020.1849440
95. Xiao Z, Luo P, Li G, et al. HPDA-based tubule-targeting nanoplateform alleviates oxidative stress and ferroptosis for the reversal of renal interstitial fibrosis. *J Nanobiotechnol*. 2025;24(1):57. doi:10.1186/s12951-025-03927-5
96. Wang X, Deng B, Yu M, et al. Constructing a passive targeting and long retention therapeutic nanoplateform based on water-soluble, non-toxic and highly-stable core-shell poly(amino acid) nanocomplexes. *Biomater Sci*. 2021;9(21):7065–7075. doi:10.1039/d1bm01246k
97. Guo Y, Wang Y, Wang B, et al. Ultrasound-responsive renal-targeted nanoparticles deliver TAK-242 to inhibit NF- κ B/NLRP3 signaling and attenuate sepsis-associated acute kidney injury. *Biomaterials*. 2025;329:123922. doi:10.1016/j.biomaterials.2025.123922
98. Zhang J, Gu L, Jiang Y, et al. Artesunate-nanoliposome-TPP, a novel drug delivery system that targets the mitochondria, attenuates cisplatin-induced acute kidney injury by suppressing oxidative stress and inflammatory effects. *Int J Nanomed*. 2024;19:1385–1408. doi:10.2147/ijn.S444076
99. Saiz ML, Lozano-Chamizo L, Florez AB, et al. BET inhibitor nanotherapy halts kidney damage and reduces chronic kidney disease progression after ischemia-reperfusion injury. *Biomed Pharmacother*. 2024;174:116492. doi:10.1016/j.biopha.2024.116492
100. Vaidya A, Moore S, Chatterjee S, et al. Expanding RNAi to kidneys, lungs, and Spleen via Selective ORgan Targeting (SORT) siRNA lipid nanoparticles. *Adv Mater*. 2024;36(35):e2313791. doi:10.1002/adma.202313791
101. Huang J, Guo J, Dong Y, et al. Self-assembled hyaluronic acid-coated nanocomplexes for targeted delivery of curcumin alleviate acute kidney injury. *Int J Biol Macromol*. 2023;226:1192–1202. doi:10.1016/j.ijbiomac.2022.11.233
102. Bauer S, Oosterwijk-Wakka JC, Adrian N, et al. Targeted therapy of renal cell carcinoma: synergistic activity of cG250-TNF and IFN γ . *Int J Cancer*. 2009;125(1):115–123. doi:10.1002/ijc.24359
103. Li R, Li Y, Zhang J, et al. Targeted delivery of celastrol to renal interstitial myofibroblasts using fibronectin-binding liposomes attenuates renal fibrosis and reduces systemic toxicity. *J Control Release*. 2020;320:32–44. doi:10.1016/j.jconrel.2020.01.017
104. Xia C, Wang J, Bu R, Hu X. Ultrasonically targeted destruction of SDF-1 nanobubbles carrying mesenchymal stem cells improves renal tubulointerstitial fibrosis. *Int J Pharm*. 2025;690:126542. doi:10.1016/j.ijpharm.2025.126542
105. Zhou L, Ye Z, Zhang E, et al. Co-delivery of dexamethasone and captopril by α 8 integrin antibodies modified liposome-PLGA nanoparticle hybrids for targeted anti-inflammatory/anti-fibrosis therapy of glomerulonephritis. *Int J Nanomed*. 2022;17:1531–1547. doi:10.2147/ijn.S347164
106. Li M, Yang L, An Y, et al. Selenium-doped carbon dots as a multipronged nanoplateform to alleviate oxidative stress and ferroptosis for the reversal of acute kidney injury. *ACS nano*. 2025;19(18):17834–17849. doi:10.1021/acsnano.5c03415
107. Sun H, He Y, Zhao Y, Wang YJ, Chen L. “Trojan Horse” delivery of gallium nanodroplets as intelligent ferroptosis inhibitors for targeted acute kidney injury therapy. *ACS Appl Mater Interfaces*. 2025;17(50):67724–67738. doi:10.1021/acsami.5c20757
108. Lee S, Suh SH, Ma SK, et al. ROS-responsive graphene-hyaluronic acid nanomedicine for targeted therapy in renal ischemia/reperfusion injury. *Theranostics*. 2026;16(2):618–636. doi:10.7150/thno.120560
109. Fang C, Cai Y, He C, Lu Y, Wang X, Cai Y. Hydroxyl-augmented gold nanorods via lactone ring-opening alleviate cisplatin nephrotoxicity through Nrf2 activation. *Biomaterials*. 2026;325:123596. doi:10.1016/j.biomaterials.2025.123596

110. Huang Y, Zheng J, Yu M. Nanoparticle transport in proximal tubules with rhabdomyolysis-induced necrosis. *Angew Chem.* 2025;64(5): e202417024. doi:10.1002/anie.202417024
111. Tan L, Lai X, Zhang M, et al. A stimuli-responsive drug release nanoplatform for kidney-specific anti-fibrosis treatment. *Biomater Sci.* 2019;7(4):1554–1564. doi:10.1039/c8bm01297k
112. Ji Y, Wang H, Liu X, et al. Targeted inhibition of pyroptosis via a carbonized nanoinhibitor for alleviating drug-induced acute kidney injury. *J Mat Chem B.* 2024;12(23):5609–5618. doi:10.1039/d4tb00382a
113. Wang X, Yang L, Wang J, et al. Silica cross-linked micelle-based theranostic system for the imaging and treatment of acute and chronic kidney injury. *ACS Appl Bio Mater.* 2023;6(3):1213–1220. doi:10.1021/acsabm.2c01077
114. Hu X, Cheng X, Shao L, et al. NIR-II light-controlled photosynthetic activation via an upconversion nanoplatform for targeted bioenergetic therapy in acute kidney injury. *J Med Chem.* 2025;68(18):19746–19766. doi:10.1021/acs.jmedchem.5c02109
115. Taghavi S, Keshkar S, Abedanzadeh M, et al. Exosome loaded in microneedle patch ameliorates renal ischemia-reperfusion injury in a mouse model. *Stem Cells Int.* 2025;2025(1):3106634. doi:10.1155/sci/3106634
116. Ren Y, Dong Y, Li Z, et al. Kidney-targeting DNA tetrahedral molecular cage synergistically inhibits acute kidney injury by clearing ROS and activating HO-1. *Biomaterials.* 2025;320:123237. doi:10.1016/j.biomaterials.2025.123237
117. Jang H, Park D, Park B, et al. Oral PTP1B siRNA delivery using milk-derived extracellular vesicles for alleviation of acute kidney injury. *ACS nano.* 2025;19(46):40085–40099. doi:10.1021/acsnano.5c15067
118. Akinleye AA, Chapman HM, Roman RJ, Bidwell GL 3rd. Kidney-specific delivery of a matrix metalloproteinase-2 inhibitory peptide fused to elastin-like polypeptide reduces proteinuria and renal fibrosis in a model of salt-sensitive hypertension. *J Pharmacol Exp Ther.* 2025;392(12):103556. doi:10.1016/j.jpets.2025.103556
119. Engel JE, Williams ML, Williams E, et al. Recovery of renal function following kidney-specific VEGF Therapy in experimental renovascular disease. *Am J Nephrol.* 2020;51(11):891–902. doi:10.1159/000511260
120. Mahdi F, Chade AR, Bidwell GL 3rd. Utilizing a kidney-targeting peptide to improve renal deposition of a pro-angiogenic protein biopolymer. *Pharmaceutics.* 2019;11(10):542. doi:10.3390/pharmaceutics11100542
121. Bidwell GL 3rd, Mahdi F, Shao Q, et al. A kidney-selective biopolymer for targeted drug delivery. *Am J Physiol Renal Physiol.* 2017;312(1):F54–f64. doi:10.1152/ajprenal.00143.2016
122. Ma W, Wu D, Long C, et al. Neutrophil-derived nanovesicles deliver IL-37 to mitigate renal ischemia-reperfusion injury via endothelial cell targeting. *J Control Release.* 2024;370:66–81. doi:10.1016/j.jconrel.2024.04.025
123. Zhao X, Sun J, Dong J, et al. An auto-photoacoustic melanin-based drug delivery nano-plattform for self-monitoring of acute kidney injury therapy via a triple-collaborative strategy. *Acta Biomater.* 2022;147:327–341. doi:10.1016/j.actbio.2022.05.034
124. Haas M, Kluppel AC, Wartna ES, et al. Drug-targeting to the kidney: renal delivery and degradation of a naproxen-lysozyme conjugate in vivo. *Kidney Int.* 1997;52(6):1693–1699. doi:10.1038/ki.1997.504
125. Xu Y, Niu Y, Wu B, et al. Extended-release of therapeutic microRNA via a host-guest supramolecular hydrogel to locally alleviate renal interstitial fibrosis. *Biomaterials.* 2021;275:120902. doi:10.1016/j.biomaterials.2021.120902
126. Chen Q, Huang J, Gou J, Ren Q, Yuan L. Inulin as carriers for renal targeting delivery of ferulic acid. *Int J Biol Macromol.* 2020;154:654–660. doi:10.1016/j.ijbiomac.2020.03.054
127. Wang Y, Liu S, Zhu F, et al. Improved bioavailability and anti-nephrotoxicity efficacy of polydatin on cisplatin-induced AKI via a dual-targeting fucoidan delivery system. *Int J Pharm.* 2025;10:100422. doi:10.1016/j.ijpx.2025.100422
128. Wang X, Liu X, Xu L, et al. Targeted delivery of type I TGF- β receptor-mimicking peptide to fibrotic kidney for improving kidney fibrosis therapy via enhancing the inhibition of TGF- β 1/Smad and p38 MAPK pathways. *Int Immunopharmacol.* 2024;137:112483. doi:10.1016/j.intimp.2024.112483
129. Widiasta A, Sribudiani Y, Nugrahapraja H, Hilmanto D, Sekarwana N, Rachmadi D. Potential role of ACE2-related microRNAs in COVID-19-associated nephropathy. *Non-Coding RNA Res.* 2020;5(4):153–166. doi:10.1016/j.ncrna.2020.09.001
130. Imig JD, Hye Khan MA, Burkhan A, Chen G, Adebisi AM, Falck JR. Kidney-targeted epoxyeicosatrienoic acid analog, EET-F01, reduces inflammation, oxidative stress, and cisplatin-induced nephrotoxicity. *Int J Mol Sci.* 2021;22(6):2793. doi:10.3390/ijms22062793
131. Zhang Y, Wang L, Yang X, et al. LRG1-targeted nintedanib delivery for enhanced renal fibrosis mitigation. *Nano Lett.* 2024;24(35):11097–11107. doi:10.1021/acs.nanolett.4c03315
132. Zhou C, Luo Z, Zhang Z, et al. Screening and identification of novel DNA aptamer for targeted delivery to injured podocytes in glomerular diseases. *Adv Sci.* 2025;12(20):e2412356. doi:10.1002/advs.202412356
133. Zhou X, Chen Q, Guo C, et al. CD44 receptor-targeted and reactive oxygen species-responsive H(2)S donor micelles based on hyaluronic acid for the therapy of renal ischemia/reperfusion injury. *ACS omega.* 2022;7(46):42339–42346. doi:10.1021/acsomega.2c05407
134. Maier H, Járos GG, van Hoorn-Hickman R, Hall A. Effects of an intravenous bolus calcium injection on glomerular filtration rate and electrolyte excretion in the kidney in conscious pigs. *South Afr Med J.* 1985;67(9):343–346.
135. Xu Y, Qin S, Niu Y, Gong T, Zhang Z, Fu Y. Effect of fluid shear stress on the internalization of kidney-targeted delivery systems in renal tubular epithelial cells. *Acta pharmaceutica Sinica B.* 2020;10(4):680–692. doi:10.1016/j.apsb.2019.11.012
136. Qin S, Wu B, Gong T, Zhang ZR, Fu Y. Targeted delivery via albumin Corona nanocomplex to renal tubules to alleviate acute kidney injury. *J Control Release.* 2022;349:401–412. doi:10.1016/j.jconrel.2022.07.013
137. Chen Z, Li W, Shi L, et al. Kidney-targeted astaxanthin natural antioxidant nanosystem for diabetic nephropathy therapy. *Eur J Pharm Biopharm.* 2020;156:143–154. doi:10.1016/j.ejpb.2020.09.005
138. Fang P, Han L, Liu C, et al. Dual-regulated functionalized liposome-nanoparticle hybrids loaded with dexamethasone/TGF β 1-siRNA for targeted therapy of glomerulonephritis. *ACS Appl Mater Interfaces.* 2022;14(1):307–323. doi:10.1021/acsmi.1c20053
139. Sabiu G, Kasinath V, Jung S, Li X, Tsokos GC, Abdi R. Targeted nanotherapy for kidney diseases: a comprehensive review. *Nephrol Dial Transplant.* 2023;38(6):1385–1396. doi:10.1093/ndt/gfac233
140. Wang Z, Zhang C. Nanomaterials for targeted therapy of kidney diseases: strategies and advances. *Mater Today Bio.* 2025;31:101534. doi:10.1016/j.mtbio.2025.101534
141. Vasyliaki A, Ghosh P, Jaimes EA, Williams RM. Targeting the kidneys at the nanoscale: nanotechnology in nephrology. *Kidney360.* 2024;5(4):618–630. doi:10.34067/kid.000000000000400

142. Funahashi Y, Park SH, Hebert JF, et al. Nanotherapeutic kidney cell-specific targeting to ameliorate acute kidney injury. *Kidney Int.* 2024;106(4):597–610. doi:10.1016/j.kint.2024.06.021
143. Hou Y, Zhu L, Ye X, et al. Integrated oral microgel system ameliorates renal fibrosis by hitchhiking co-delivery and targeted gut flora modulation. *J Nanobiotechnol.* 2024;22(1):305. doi:10.1186/s12951-024-02586-2

International Journal of Nanomedicine

Publish your work in this journal

The International Journal of Nanomedicine is an international, peer-reviewed journal focusing on the application of nanotechnology in diagnostics, therapeutics, and drug delivery systems throughout the biomedical field. This journal is indexed on PubMed Central, MedLine, CAS, SciSearch[®], Current Contents[®]/Clinical Medicine, Journal Citation Reports/Science Edition, EMBase, Scopus and the Elsevier Bibliographic databases. The manuscript management system is completely online and includes a very quick and fair peer-review system, which is all easy to use. Visit <http://www.dovepress.com/testimonials.php> to read real quotes from published authors.

Submit your manuscript here: <https://www.dovepress.com/international-journal-of-nanomedicine-journal>

Dovepress
Taylor & Francis Group